의학박사 학위논문

Radiosensitization of Glioblastoma Cells by a Novel DNA Methyltransferase-Inhibiting Phthalimido-Alkanamide Derivative

교모세포종 세포주 및 이식종양 모델에서 DNA Methyltransferase 억제제인 신합성 Phthalimido-alkanamide 유도체의 방사선감수성 증강효과 및 기전

2019년 8월

서울대학교 대학원

의학과 방사선종양학 전공

위 찬 우

Abstract

Radiosensitization of Glioblastoma Cells by a Novel DNA Methyltransferase-Inhibiting Phthalimido-Alkanamide Derivative

Chan Woo Wee

Medicine (Radiation Oncology Major)

The Graduate School

Seoul National University

Background and purpose: Radiotherapy is an essential element for treating glioblastoma, the most common malignant adult brain tumor harboring devastating prognosis. Strategies to enhance the therapeutic ratio of radiotherapy in glioblastoma are warranted. Our aim is to report a novel DNA methyltransferase inhibitor as a potential radiosensitizing agent in glioblastoma.

Materials and Methods: Four glioblastoma cell lines (U87MG, U373MG, U138MG, and T98G) and one normal astrocyte cell line (NHA) were used. Radiosensitizing effects of a newly synthesized phthalimido-alkanamide derivative, MA17, were assessed in these cells using clonogenic assay. 6MV X-rays were used for irradiation of cells and pretreatment with MA17 was done for cells treated by combined treatment. We performed a tumor growth delay assay with two glioblastoma lines (U87MG and U138MG) using BALB/C-nude mice. We also evaluated DNA methyltransferase

(DNMT) inhibition, apoptosis, autophagy, DNA damage repair, and FANCA expression. Tissue-to-plasma partition coefficient of MA17 was obtained to evaluate blood-brain barrier penetration and distribution in brain tissues.

Results: MA17 significantly radiosensitized all glioblastoma cells *in vitro* with mean sensitizer enhancement ratios of 1.196 ($p=0.034$), 1.441 ($p=0.029$), 1.152 ($p=0.030$), and 1.350 ($p<0.001$) at a surviving fraction of 0.2 for U87MG, U373MG, U138MG, and T98G cells, respectively. However, MA17 did not affect the radiosensitivity of NHA cells with mean sensitizer enhancement ratio of 1.016 ($p=0.420$). The mean tumor doubling time *in vivo* in cells treated with irradiation+MA17, compared to irradiation alone, was prolonged by a margin of 6.35 days ($p=0.009$) and 3.06 days ($p=0.030$) in U87MG and U138MG cells, respectively. Western blotting revealed that DNMT1/DNMT3A/DNMT3B activity is down-regulated, and apoptosis/autophagy are induced by MA17. Double-stranded DNA break foci were observed for prolonged periods in cells treated with MA17 in all 4 glioblastoma cell lines. FANCA expression was also inhibited by MA17. The tissue-to-plasma partition coefficient was unquantifiable indicating inability of MA17 to cross the blood-brain barrier.

Conclusion: We first evaluated a novel phthalimido-alkanamide derivative, MA17, as a potential radiosensitizer in human glioblastoma cells. MA17 demonstrated significant radiosensitization in glioblastoma cells *in vitro* and *in vivo*. Radiosensitization was associated with induction of apoptosis and autophagy, as well as suppression of DNA damage repair and FANCA expression. Further investigation is needed to translate these results to the clinic.

Keywords: DNA methyltransferase, irradiation, radiosensitizer, glioblastoma,

phthalimido-alkanamide

Student number: 2014-21992

Contents

List of Tables

List of Figures

Introduction

Glioblastoma (GBM) is the most common primary malignant brain tumor consisting nearly half of all histologies with a high mortality rate (1). The initiation of the treatment for this notorious brain tumor is by maximal safe resection and histologic confirmation. Adjuvant treatment is usually recommended in the clinics depending on the expected survival of patient. Ever since Walker et al., on behalf of the Brain Tumor Study Group, demonstrated that radiotherapy (RT) significantly improves survival in GBM patients over best supportive care or 1,3-bis(2-chloroethyl)-l-nitrosourea chemotherapy alone, RT has been the only crucial treatment following surgical resection or biopsy for several decades (2). In 2005, the practice changing report by Stupp et al. enabled the use of concurrent and adjuvant temozolomide combined with RT, and this remains the standard of care to date (3).

Despite standard chemoradiation with RT and temozolomide, GBM patients present a devastating median survival of 15–20 months (3, 4). The prognosis of the disease becomes even more dismal for patients with older age with a median survival of 9 months (5). Furthermore, especially in tumors with an unmethylated O^6-methylguanine–DNA methyltransferase (*MGMT*) promoter, the outcome is further reduced by poor response to standard chemoradiation (4) emphasizing the effect of epigenetic changes on the outcome of the disease. However, no drug has been successful in improving the overall survival outcome for GBM as first-line treatment for nearly 15 years. For example, modification of the dosage-dense of temozolomide during the adjuvant period following chemoradiation resulted in a statistically equivalent

overall survival compared to the standard-dose group (3) with both arm demonstrating a median survival of 15–16 months in the RTOG-0525 study by Gilbert et al (6). A monoclonal antibody inhibiting vascular endothelial growth factor A, bevacizumab, which is one of the mostly commonly agents for recurrent GBM, have also failed to improve overall survival as first-line therapy. In the RTOG-0825 trial, when added to standard chemoradiation (3), the overall survival remained 16 months, which was identical between the control and experimental arm (7). Novel agents are urgently needed for the sake of GBM patients.

In fact, GBM is considered somewhat radioresistant in various ways, and the underlying mechanism are being widely investigated in order to overcome the unconditional recurrence of GBM after RT (8–10). Most of these failures after RT tend to occur 'in-field', the targeted area of previous irradiation (12, 13). Minniti et al (12), examined 132 GBM patients treated with 3-dimensional conformal RT and standard temozolomide (3), of which 105 patients developed recurrence. Eighty-percent of those recurrences were 'central', indicating that over 95% of the volume of the recurred tumor lied in the high-dose region irradiated up to 60 Gy according to the predefined definition (12). Tumors with unmethylated *MGMT* promoters showed significantly higher tendency of 'central' recurrence compared to tumors with methylated *MGMT* promoters, although 'central' recurrence was predominant in both subtypes in concordance with the finding from RTOG-0525 (4, 11). A study from MD Anderson Cancer Center by Chang et al. also reported a similar result in 48 GBM patients where all of them experienced disease recurrence (13). Ninety-percent of patients

demonstrated centrally leading to a conclusion that wider margins or routine inclusion of peritumoral edema are not necessary for achieving better disease control and they only result in excessive irradiation of the normal brain (13). This indicates the feasibility of focusing on the gross tumor observed in the magnetic resonance. All together, these findings suggest that novel strategies to increase the local tumor control probability of RT while maintaining or reducing the current toxicity profiles of normal brain tissues, such as radiosensitizing the GBM cells, are necessary.

Epigenetic aberrations, such as DNA methylation and histone protein modifications, are critical for carcinogenesis and cancer growth (14, 15). DNA methylation is the most widely investigated epigenetic aberration in cancer. Particularly, 5-methylcytosine is resulted by methylation at the fifth position of cytosines at CpG sites. DNA methyltransferases (DNMTs) mediate the introduction of a methyl-group (CH3) at cytosine bases (16, 17). Although global hypomethylation can also be observed in cancers, most cancer cells harbor hypermethylated CpG islands in their DNA. Furthermore, critical biological pathways in gliomas, such as the p53 or retinoblastoma pathways, are known to be affected by the hypermethylation of CpG islands (18, 19). Changes in promoter DNA methylation profiles of other key pathways are also well studied in GBM. Methylation of the *MGMT* promoter is probably the most clinically impactful epigenetic alteration in newly diagnosed GBM. Not only is it clinically reliable in predicting the prognosis after treatment as aforementioned (3, 4), it is the most reliable factor to predict the treatment-response to temozolomide-based chemoradiation (20). Epigenetic silencing of

the *MGMT* DNA repair gene, located on chromosome 10q26, leaves tumor cells with unremoved alkyl groups from O^6-methylguanine lesions induced by alkylation formed by temozolomide, eventually resulting in increased cytotoxicity and apoptosis. Another representative finding of epigenetic DNA methylation in GBM is the identification of the glioma-CpG island methylator phenotype (G-CIMP) using The Cancer Genome Atlas dataset (21). Based on DNA methylation profiles, Noushmehr et al. found a group of tumors (8.8%) showing similar hypermethylation at a subset of loci, and designated them as the G-CIMP (21). Patients with G-CIMP subtype were characterized by younger age and a higher incidence of mutated IDH1 gene. Strikingly, proneural G-CIMP-positive patients demonstrated an unusual long-term survival of median >10 years, which was significantly longer compared to the proneural G-CIMP-negative and nonproneural subtypes, resembling that of low-grade gliomas. Overall, methylation of gene promoters is an epigenetic change significantly influencing the biological behavior, prognosis, and response to treatment in GBM.

Moreover, given the frequent overexpression of DNMT in cancer, DNMT inhibitors (DNMTis) have been widely investigated as potential targets of anti-cancer therapy. For acute myeloid leukemia, hypermethylation of tumor suppressor genes is related to carcinogenesis and poor prognosis. Targeting this hypermethylation, two nucleoside analogue DNMTs, 5-azacytidine (Azacitidine, Vidaza®) and 5-aza-2'-deoxycytidine (Decitabine, Dacogen®), have been already approved by the FDA for its anticancer activity and are being used in the clinics nowadays (22). However, the efficacy of nucleoside DNMTis

as cancer treatment has occasionally been dampened due to toxicity and poor chemical stability. Therefore, development of non-nucleoside DNMTis is needed.

Not only as direct anticancer drugs itself, DNMTis have been shown to enhance lethality to radiation, an effect so-called 'radiosensitization', in various human cancer cell lines (23–27). Our previous study showed that psammaplin A, decitabine, and zebularine radiosensitize both human lung cancer and glioblastoma cells by inhibiting DNA repair (23). Hofstetter B and colleagues demonstrated that hypomethylation of genes by azacitidine can increase the radiosensitivity in colorectal cell lines (24). Gastric cancer cells were also shown to be radiosensitized by 5-aza-2'-deoxycytidine (25). Our previous study showed that psammaplin A, decitabine, and zebularine radiosensitize both human lung cancer and glioblastoma cells by inhibiting DNA repair (23). However, further application of the non-nucleoside DNMTi psammaplin A *in vivo* was hindered due to its poor biostability despite its radiosensitizing efficacy (28). For this reason, we have been investigating the application of non-nucleoside DNMTis with respect to their radiosensitizing effect as well as their biostability. We have synthesized over 20 compounds based on the backbone of psammaplin A or with few modifications. However, our previous study failed to increase biostability although the radiosensitizing effect was maintained in the majority of compounds (29).

Recently, we synthesized a novel phthalimido-alkanamide derivative (undisclosed formula, $C_{26}H_{30}N_2O_5$), at the College of Pharmacy, in the Catholic University of Daegu, using a phthalimid backbone (PubChem Compound ID:

6809). The compound was nomenclature ‘MA17’. In our previous study using human lung adenocarcinoma cells, MA17 was shown to radiosensitize the cells by inhibiting DNA repair, especially by suppressing the homologous recombination and the Fanconi anemia DNA repair pathway (30). Here we present the *in vitro* and *in vivo* results from GBM cell lines of MA17.

Materials and Methods

1. MA17 and cell culture

When 6-week old albino male ICR mice (n=4) were injected with 10 mg/kg of MA17, this showed good bioavailability with an elimination half-life of 1.0±0.2 hour (Catholic University of Daegu IACUC No. 2016-007) (Table 1). MA17 was dissolved in DMSO at a concentration of 20 mM and was stored at room temperature. Four human GBM cell lines (U87MG, U373MG, U138MG, and T98G) and one normal human astrocyte (NHA) cell line were used in this study. U87MG/U373MG cells (Korean Cell Line Bank, Seoul, Korea) and U138MG/T98G/NHA (American Type Culture Collection, Manassas, USA) cells were cultured and maintained in RPMI 1640 and DMEM media, respectively (Welgene, Daegu, Korea), at 37˚C with 5% (v/v) CO2. Media were supplemented with 10% fetal bovine serum (Gibco, Grand Island, US) with an added 12.5 μg/ml of gentamicin (Gibco). U87MG and U373 cells represent GBM cells with methylation in the *MGMT* promoter, whereas U138MG and T98G cells have an unmethylated *MGMT* promoter in the current study (31–33).

Table 1. Pharmacokinetic parameters after intravenous injection of compound MA17 at a dose of 10 mg/kg (n=4).

Parameters	Mean	±	SD
$t_{1/2}$, λn (hour)	1.0	±	0.2
C_0 (ng/mL)	6458.2	±	1818.2
AUC_{all} (ng·hr/mL)	941.3	±	206.7
AUC_{inf} (ng·hr/mL)	947.5	±	205.2
CL (mL/min/kg)	184.0	±	49.9
V_{SS} (L/kg)	3.3	±	2.1

SD: standard deviation; $t_{1/2}$: the average terminal elimination half; C_0: the concentration at the beginning of observation; CL: the systemic clearance; AUC: the area under the curve; V_{SS}: the volume of distribution at steady state.

2. Clonogenic assay

Cell survival after RT±MA17 was measured using the clonogenic assay as previously reported (23). Cells were trypsinized from the growing monolayer cultures, and the planned number of cells were seeded into T25 flasks and were incubated for 24 h prior RT. For RT, 6 megavoltage (MV) photon beams were used at doses of 0–8 Gy (Clinac 21iX Silhouette, Varian Medical Systems, Palo Alto, USA). For RT+MA17, MA17 was administered for 24 hours prior to RT. Following treatment, cells were incubated for 14 days to allow for colony formation. Colonies containing ≥50 cells were counted after fixation with methanol and staining with 0.5% crystal violet. All experiments were done in triplicates.

3. Tumor growth delay assay

Tumor growth delay assays were performed *in vivo* using the U87MG and U138MG cell lines, under the approval of the Seoul National University Hospital (IACUC No. 16-0016-C1A1). Tumor cells (2×10^6) in 100 μl of media supplemented with fetal bovine serum were injected intradermally in the back of 6-week old female BALB/C-nude mice (Orient, Seongnam-si, Korea) irrespective of their weight. The mean weight of mice was 18.19±0.92 g. U87MG and U138MG cells were transferred in RPMI and DMEM media, respectively, and were supplemented with 15% fetal bovine serum. When the mean tumor volume reached 450 mm^3 for U87MG and 300 mm^3 for U138MG, mice were randomly placed into four groups: i) control (arm 1, n=5), ii) RT (arm 2, n=5), iii) MA17 (arm 3, n=5), and iv) RT+MA17 (arm 4, n=5).

After randomizing the mice in the aforementioned groups, RT was delivered to mice in arms 2 and 4. In each mouse, one fraction of 8-Gy was delivered to the tumor at a dose rate of 300 monitor units/min using 6-MV electron beams. The back of the mouse was covered with 1-cm tissue-equivalent bolus to ensure the coverage of the superficial portion of the tumors. Vehicle or MA17 was delivered twice intraperitoneally 45 minutes pre-RT and post-RT. The vehicle consisted of 477.78 μL phosphate-buffered saline and 22.22 μL DMSO for each injection, whereas the drug for arms 3 and 4 consisted of 3-mg MA17 dissolved in the identical solution. Therefore, mice in arms 3 and 4 received a total MA17 of 6 mg each. Starting from the first day of the treatment, the tumor volume was measured every 2-3 days, using a digital caliper (Digimatic Caliper CD-15CPX, Mitutoyo Corporation, Kawasaki, Japan) and was calculated using the formula of {(length × width × height) × π}/6. Tumor doubling time (TBT) was used to compare the tumor growth between treatment arms. To assess acute toxicity of treatment, we assessed the weight (g) of each mouse as well as unexpected mortality for the first 3 weeks after treatment.

4. DNMT1 colorimetric assay

A quantitative assay for the DNMT1 inhibitory activity of MA17 was performed using the colorimetric EpiQuik DNMT activity/inhibition assay Ultra kit (catalog No. P-3009, Epigentek, Farmingdale, USA) and 100 ng of DNMT1 proteins (catalog No. E-15000, Epigentek), according to the manufacturer's instructions. The DNMT1 activity was proportional to the

sample optical density (OD). The DNMT1 inhibition was calculated as follows: DNMT1 inhibition (%) = [1 – (inhibitor sample OD – blank OD)/(no inhibitor sample OD – blank OD)] ×100. Data were obtained from triplicate experiments.

5. Western blotting

The expression of each target protein was compared to that of β-actin by densitometric analysis, using the ChemiDoc Touch Image Lab (Bio-Medical Science Co., Seoul, Korea). To evaluate the inhibitory effect of MA17 on DNMT1, DNMT3A, and DNMT3B, comparisons of these proteins' expressions were performed between cells treated with and without MA17 for 24 hours. The expression of cleaved caspase-3 (antibody from Cell Signaling Technology, Danvers, MA, US) was examined to evaluate apoptosis. Western blotting for DNMT1, DNMT3A, DNMT3B, and cleaved caspase-3 expression was performed as previously reported (23).

To investigate how MA17 affects autophagy, we selected 2 target proteins, LC3B and Beclin-1, which are known to accurately represent autophagosome formation (34). LC3-I to LC3-II conversion is an indicator of autophagic activity in mammals, represented by the LC3-II to LC3-I ratio (21). Primary antibodies against LC3B (1:1000; catalog No. 3868; Cell Signaling Technology) and Beclin-1 (1:1000; catalog No. 3495; Cell Signaling Technology) were used. Cleaved caspase-3, LC3-II to LC3-I ratio, and Beclin-1 expression was examined and compared between cells treated with MA17 for 24 h prior to RT at these times post-RT: i) 0.5, ii) 6, iii) 24, and iv) 48 h and untreated cells. RT consisted of 6 Gy in a single fraction using 6 MV photons.

In a separate experiment from our lab using human lung adenocarcinoma cells (A549, Korean Cell Line Bank) and next generation sequencing, cells treated with RT+MA17 showed a significant down-regulation in the Fanconi anemia pathway, specifically in the regulation of the FANCA gene, compared to those treated by RT alone (30). Fanconi anemia pathway is known as one of the key pathways for the repair of DNA double-strand breaks (35). Therefore, to validate the additional inhibition of FANCA gene and the Fanconi anemia pathway by MA17, we evaluated the expression of FANCA proteins in the four GBM cells in a timely manner as above by western blotting (n=1 for each cell).

When MA17 was used for western blot, the pretreatment with 24 hour with the respective 50% inhibitory concentrations for each cell line was done.

6. Immunocytochemistry

Immunocytochemistry was performed as described previously using the DAPI nuclear counterstain and a FITC-labeled secondary antibody (Invitrogen, Camarillo, US) (23). Evaluated timepoints were post-RT 0.5, 6, 24, and 48 hours. Slides were examined using a confocal laser scanning microscope (LSM 800, Carl Zeiss, Oberkochen, Germany). Images were acquired using the acquisition software ZEN 2.3 (blue edition) (Carl Zeiss). Proportion of cells harboring >10 γH2AX foci were counted to examine DNA double-strand breaks over time. A single fraction of 6-Gy was delivered for all cells.

7. Tissue distribution of MA17 *in vivo*

To assess whether MA17 is able to penetrate across the blood-brain

barrier (BBB) and can distribute in the normal brain tissue *in vivo*, 6-week old albino male ICR mice were used (n=3). They were injected with 10 mg/kg of MA17 intravenously (Catholic University of Daegu IACUC No. 2016-007). The tissue-to-plasma partition coefficient (K_p), an indicator of the extent of tissue distribution of a compound, was obtained for brain, lung, testis, spleen, liver, and kidney at post-injection 1.5 hours.

8. KEGG pathway analysis

U373MG cells were treated with RT or RT+MA17. For U373MG cells treated by RT+MA17, pretreatment with MA17 for 24 hours prior to RT was done using the 50% inhibitory concentration of 120 μM. Samples were obtained at serial timepoints as follows: post-RT 0.5, 6, and 24 hours. Detailed RNA isolation and sequencing were performed as previously described (30).

Differentially expressed genes between U373MG cells treated with RT vs. RT+MA17 were identified at each time point with a cutoff log-fold change >1.0. These gene sets were mapped to the Kyoto Encyclopedia of Genes and Genomes (KEGG) pathways using the 'KEGG Mapper'. Since MA17 was hypothesized to suppress the DNA repair processes of tumor cells (30), we focused on five DNA repair-specific pathways as follows: the base excision repair, mismatch repair, homologous recombination, non-homologous end-joining, and the Fanconi anemia pathways. related to the five DNA repair pathways.

9. Statistical analysis

The graphic and data analysis application KaleidaGraph, version 3.51 (Synergy Software, Reading, USA), was used to fit the surviving fractions to a linear quadratic model. From this model, parameters were obtained to calculate the required dose to achieve a surviving fraction of 0.2. Then, to evaluate the radiosenstitizing effect of MA17 *in vivo*, a one-tailed ratio paired t-test was used between the required radiation doses to achieve the specified surviving fraction. Sensitizer enhancement ratio (SER) was obtained using the following formula: SER = (RT dose required for surviving fraction 0.2 without MA17) ÷ (RT dose required for surviving fraction 0.2 with MA17). In the tumor growth delay assay, the one-tailed Mann–Whitney test was used to compare the mean TBTs between arms 1, 2, 3, and 4. All statistical analyses were performed using the Statistical Package for Social Sciences, version 23.0 (IBM Corp., Armonk, USA). It was considered statistically significant when the p-value was below 0.05. All results are presented as a mean±standard deviation, unless specified differently.

Results

1. Radiosensitization *in vitro*

The 50% inhibitory concentrations of MA17, which is the concentration of MA17 needed to kill half of the cells, were 171.81±22.82, 108.29±29.96, 774.86±57.59, 246.17±75.06, and 324.66±44.55 μM in U87MG, U373MG, U138MG, T98G, and NHA cells, respectively. Therefore, in the assays that followed, we established a MA17 concentration of 150, 120, 750, 250, and 300 μM for using in U87MG, U373MG, U138MG, T98G, and NHA cells, respectively.

MA17 was shown to significantly radiosensitize all four human GBM cell lines with the 50% inhibitory doses mentioned above, however, it did not affect the radiation sensitivity of NHA cells (Figure 1). The mean SERs of MA17 at a surviving fraction of 0.2 in U87MG, U373MG, U138MG, T98G, and NHA cells were 1.196 ($p=0.034$), 1.441 ($p=0.029$), 1.152 ($p=0.030$), 1.350 ($p<0.001$), and 1.016 ($p=0.420$), respectively.

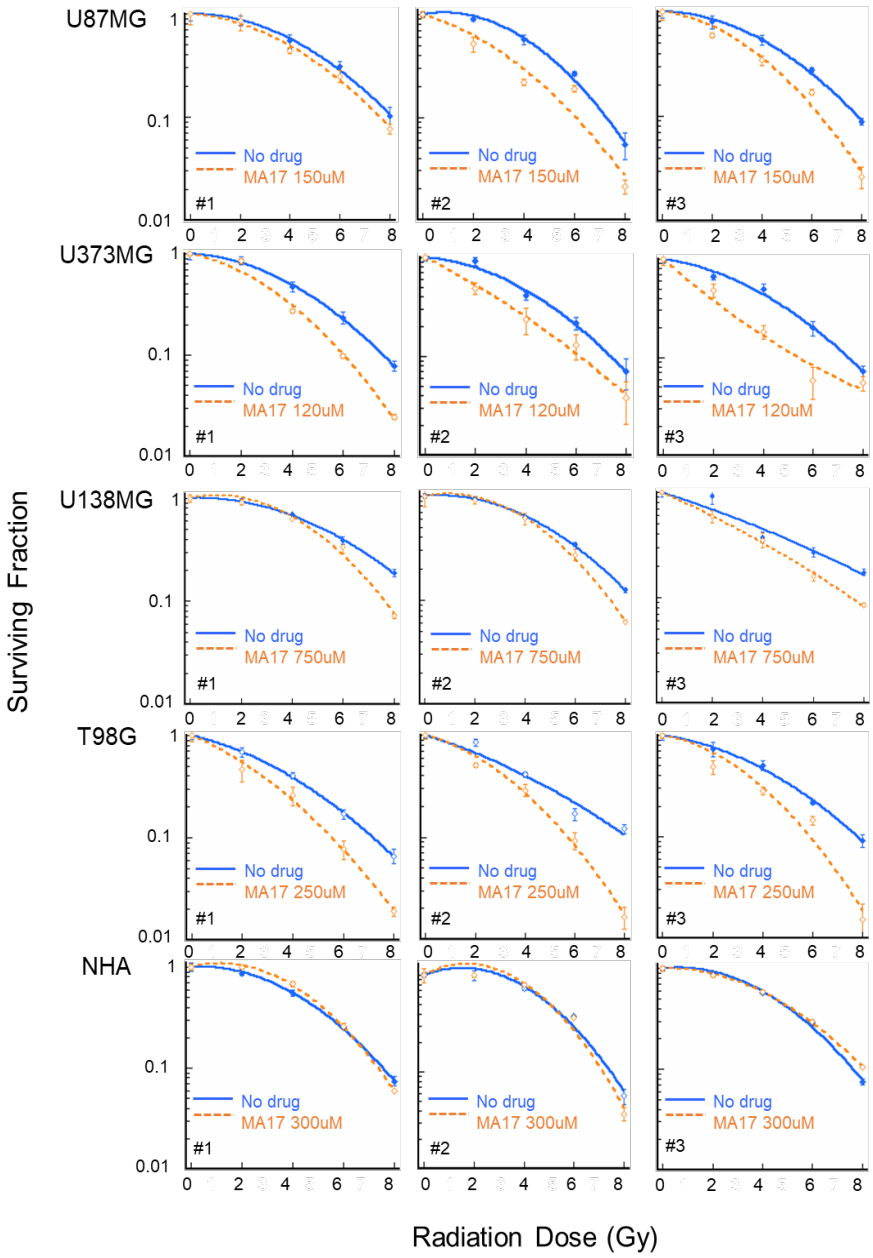

Figure 1. Clonogenic cell survival in four glioblastoma cell lines and in NHA cells following radiotherapy combined with or without MA17. Cells were treated with or without MA17, using concentrations determined as 50% inhibitory concentration, for 24 hours before radiotherapy with graded doses of X-ray. For each cell line, radiosensitization was evaluated in triplicates, and for

every respective evaluation, surviving fractions were calculated and shown as mean±standard deviation by triplicate experiments. Radiosenzitivity was significantly enhanced in all four glioblastoma cell lines by MA17, whereas the radiosensitivity of normal human astrocytes were not affected.

2. Radiosensitization *in vivo*

Tumor growth curves starting on the day of randomization and treatment are displayed in Figure 2. The mice harboring U138MG cells were observed for a shorter time period and were sacrificed earlier, since the tumor grew faster than the U87MG cells. In mice with U87MG cells the mean TDT measured was 6.51±5.73, 12.25±2.96, 11.50±9.19, and 18.60±4.84 days for arms 1, 2, 3, and 4, respectively (arm 1 vs. arm 2, p=0.071; arm 1 vs. arm 3, p=0.088; arm 1 vs. arm 4, p=0.007; arm 2 vs. arm 3, p=0.312; arm 2 vs. arm 4, p=0.009; arm 3 vs. arm 4, p=0.054) (Figure 3A). The mean TDT was significantly longer in arm 4 compared to arm 2 with a margin of 6.35 days (Figure 3A).

In mice harboring U138MG cells the mean TDT was 3.67±1.09, 8.26±2.31, 4.63±1.19, and 11.32±1.56 days in arms 1, 2, 3, and 4, respectively (arm 1 vs. arm 2, p=0.007; arm 1 vs. arm 3, p=0.126; arm 1 vs. arm 4, p=0.002; arm 2 vs. arm 3, p=0.014; arm 2 vs. arm 4, p=0.030; arm 3 vs. arm 4, p=0.002) (Figure 3B). The mean TDT was significantly prolonged in arm 4 with the addition of MA17 by 3.06 days, as compared to arm 2 (Figure 3B).

There was no unexpected mortality in mice within the first month after treatment. The mean weight loss during the first 3 days following treatment was 0.97g and 0.06g in mice harboring U87MG and U138MG cells, respectively. In the U87MG-injected mice, the mean weight of mice slightly decreased during the first 3 days of treatment and gradually re-increased by time (Figure 4A). The mean weight loss for control, RT, MA17, RT+MA17 groups were 0.25g, 1.26g, 1.08g, and 1.27g, respectively. In the U138MG-injected mice, the mean weight loss during the first 3 days after treatment was only 0.06g, and it

continuously increased during observation (Figure 4B).

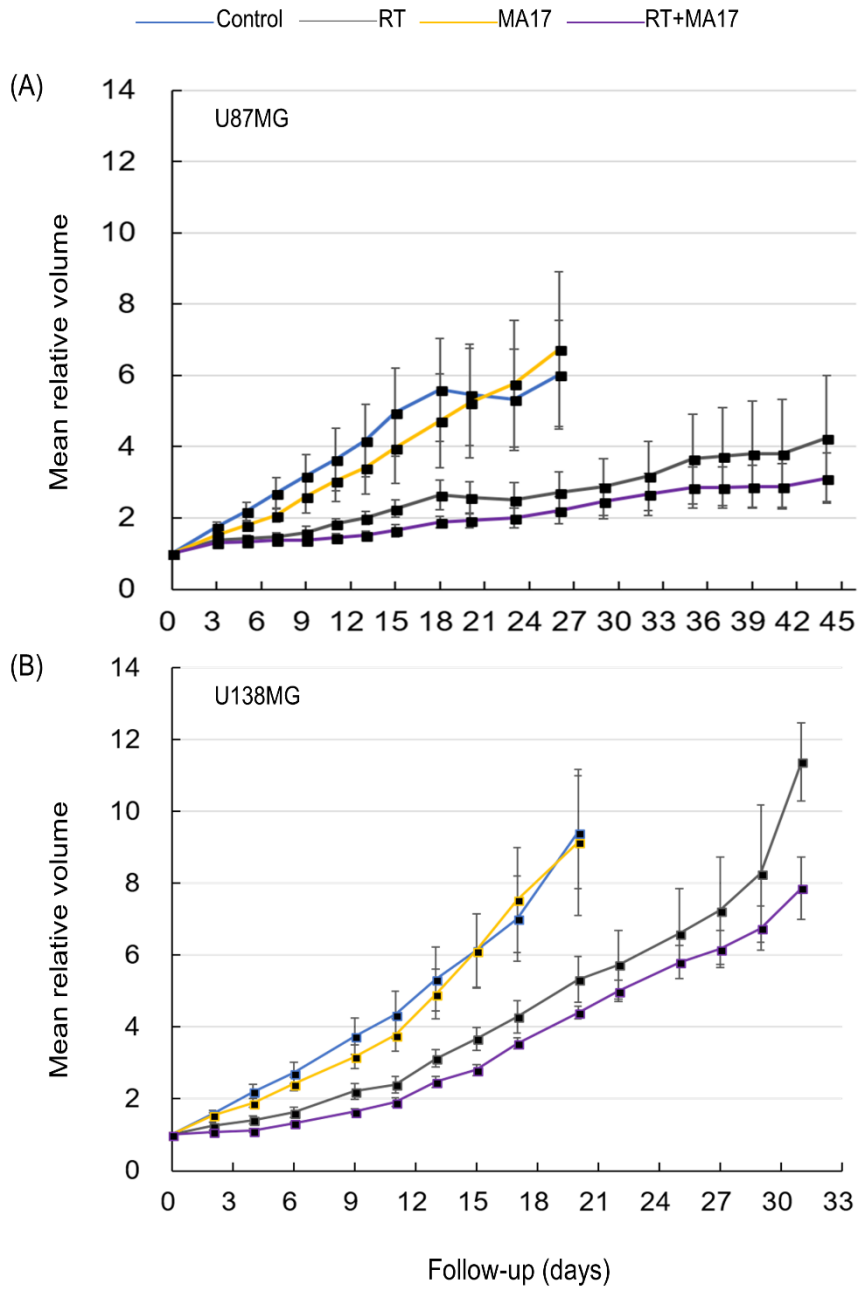

Figure 2. Tumor growth curves of U87MG and U138MG after treatment in BALB/C-nude mice. Tumor volumes are presented as relative volumes when the volume on the day of treatment is normalized to 1. On the day of randomization, the mean tumor volume of U87MG and U138MG was 450 mm^3

and 300mm^3, respectively. U138MG cells, which possess unmethylated *MGMT* promoter, were randomized and treated at a smaller volume compared to U87MG due to their rapid growth. On the tumor growth curves, tumors treated with RT demonstrated slower tumor growth compared to the tumors in the control or MA17 group. When MA17 was combined with RT, the increased in tumor size was further suppressed compared to tumors treated with RT alone. RT, radiotherapy. Error bar: Standard error. Blue line, control; gray line, RT; yellow line, MA17; purple line, RT+MA17.

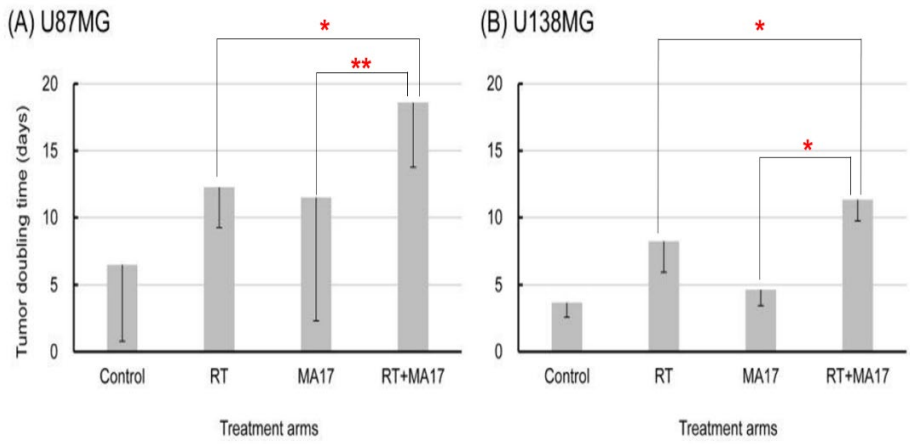

Figure 3. Mean tumor doubling times of (A) U87MG and (B) U138MG *in vivo* by treatment arms. The tumor doubling time was increased in tumors treated with RT+MA17 in both cell lines compared to those treated by either RT or MA17 alone. Although statistical significance was marginal in U87MG cells when compared RT+MA17 vs. MA17, the difference in mean tumor doubling time was 7.1 days. RT, radiotherapy. Error bar: standard deviation. $^{*}p<0.05$; $^{**}p=0.054$ by Mann-Whitney test, one-tailed.

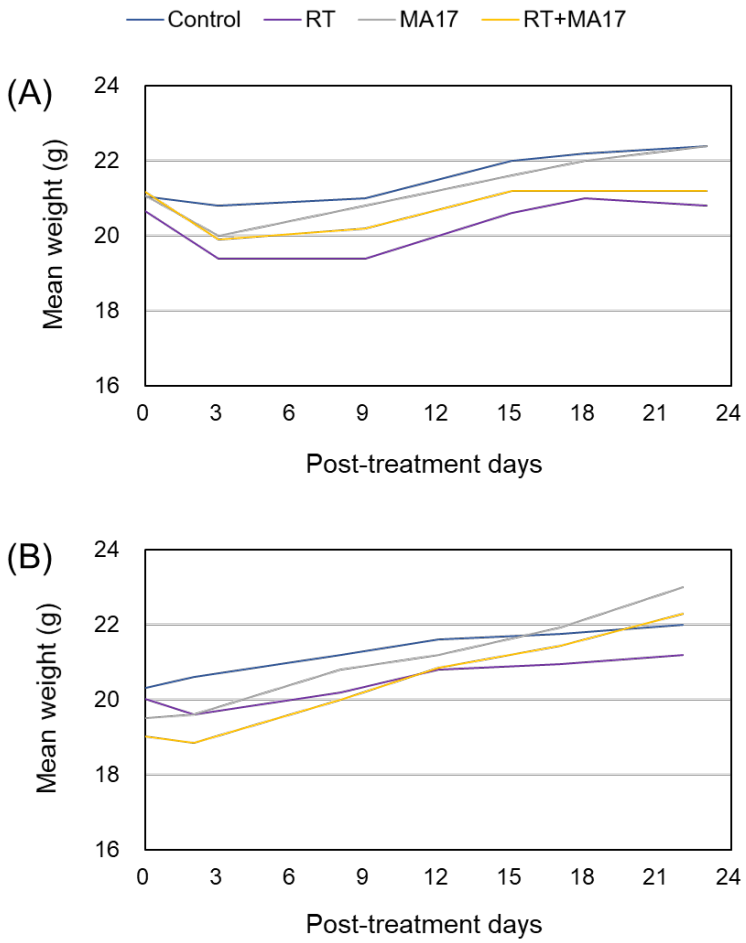

Figure 4. Changes in mean weight after treatment in mice harboring (A) U87MG and (B) U138MG cells. Both mice did not show unexpected mortality during observation. (A) Mean weight loss of 0.97g was observed during the first 3 days following treatment in U87MG-harboring mice. The weight consistently increased by time afterwards. (B) In U138MG-harboring mice, a mean weight loss of only 0.06g was observed at post-treatment 3 days. In U138MG, weight gradually increased by time as well.

3. DNMT inhibition

According to the colorimetric assay, DNMT1 activity was inhibited by 60.29±28.22% when MA17 was used. Western blotting confirmed that the expression of DNMT1, DNMT3A, and DNMT3B proteins was inhibited in all four GBM cell lines by MA17, as compared to vehicle control treatment (Figure 5).

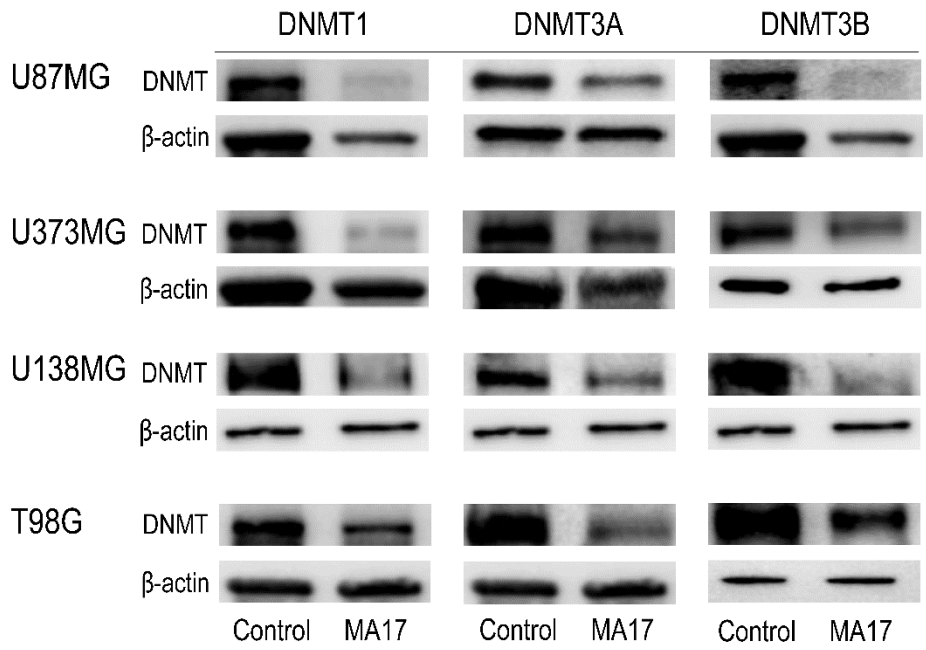

Figure 5. Western blot results of DNMT 1, DNMT3A, and DNMT3B in 4 glioblastoma cell lines after treatment with or without MA17. Protein expression of DNMT1, DNMT3A, and DNMT3B were all reduced by MA17 in U87MG, U373MG, U138MG, T98G cells. DNMT, DNA methyltransferase.

4. Apoptosis and autophagy

Evaluation of cleaved caspase-3 expression by western blotting revealed that early apoptotic tumor cell death between 0.5-24 h post-RT was significantly higher in U87MG and U373MG cells treated with RT+MA17, as compared to those receiving RT alone (Figure 6). In contrast, in U138MG and T98G cells, although cleaved caspase-3 expression levels were still higher when cells were treated with RT+MA17, compared to those not receiving MA17, the difference was only noticeable during a later phase of 24-48 h post-RT (Figure 6).

The densitometric analyses of LC3-II/LC3-I ratio and Beclin-1 expression are displayed in Figure 6. In U87MG and U373MG cells the addition of MA17 increased the LC3-II/LC3-I ratio and the Beclin-1 expression at an early phase of 0.5-6 hours post-RT (Figure 7). In U138MG cells and T98G cells the LC3-I to LC3-II ratio did not differ between cells treated by RT compared to RT+MA17, and was not consistent throughout the triplicate repeats, whereas the expression of Beclin-1 protein was higher in cells receiving MA17 at post-RT 24–48 hours.

(A)

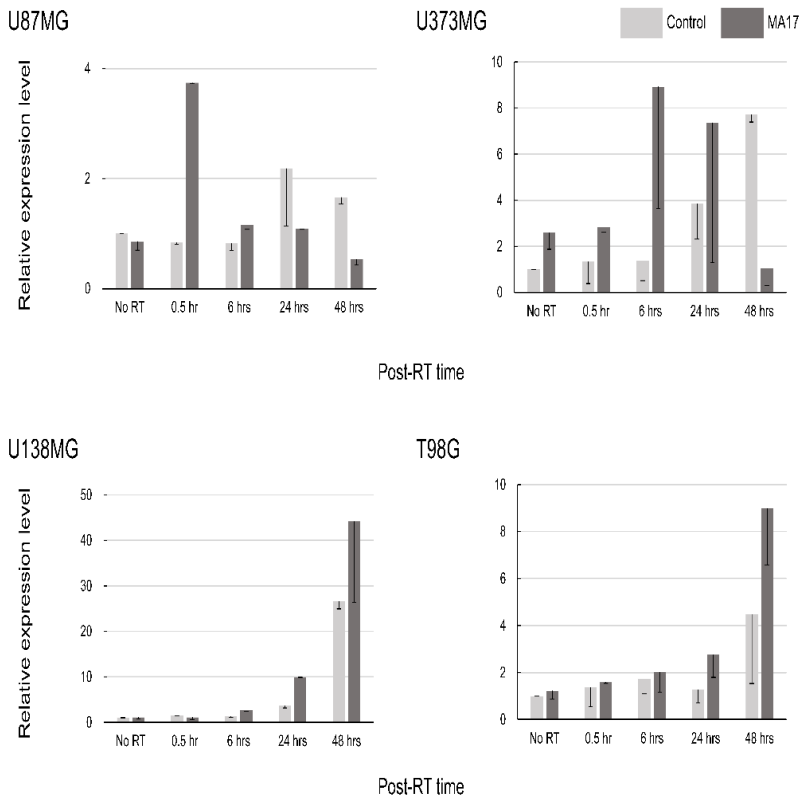

(B)

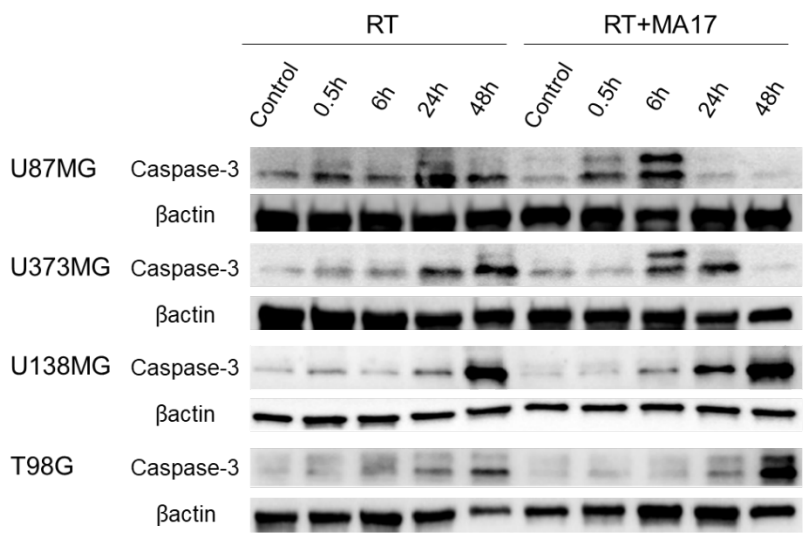

Figure 6. Western blot results for cleaved caspase-3 expression normalized to β-actin in four glioblastoma cell lines treated with RT±MA17 shown as

(A) densitometric analysis and (B) graphical protein expression bars. Cells treated with RT+MA17 demonstrated increased apoptosis in all 4 glioblastoma cells compared to cells treated with RT alone. For U87MG and U373MG, apoptosis was induced at post-RT 0.5–6 hours. Inr U138MG and T98G cells, apoptosis was increased at a delayed phase of post-RT 24–48 hours. RT, radiotherapy. Light gray bar, RT; Dark gray bar, RT+MA17 (for figure 5A). Error bar: standard deviation (for figure 5A).

(A)

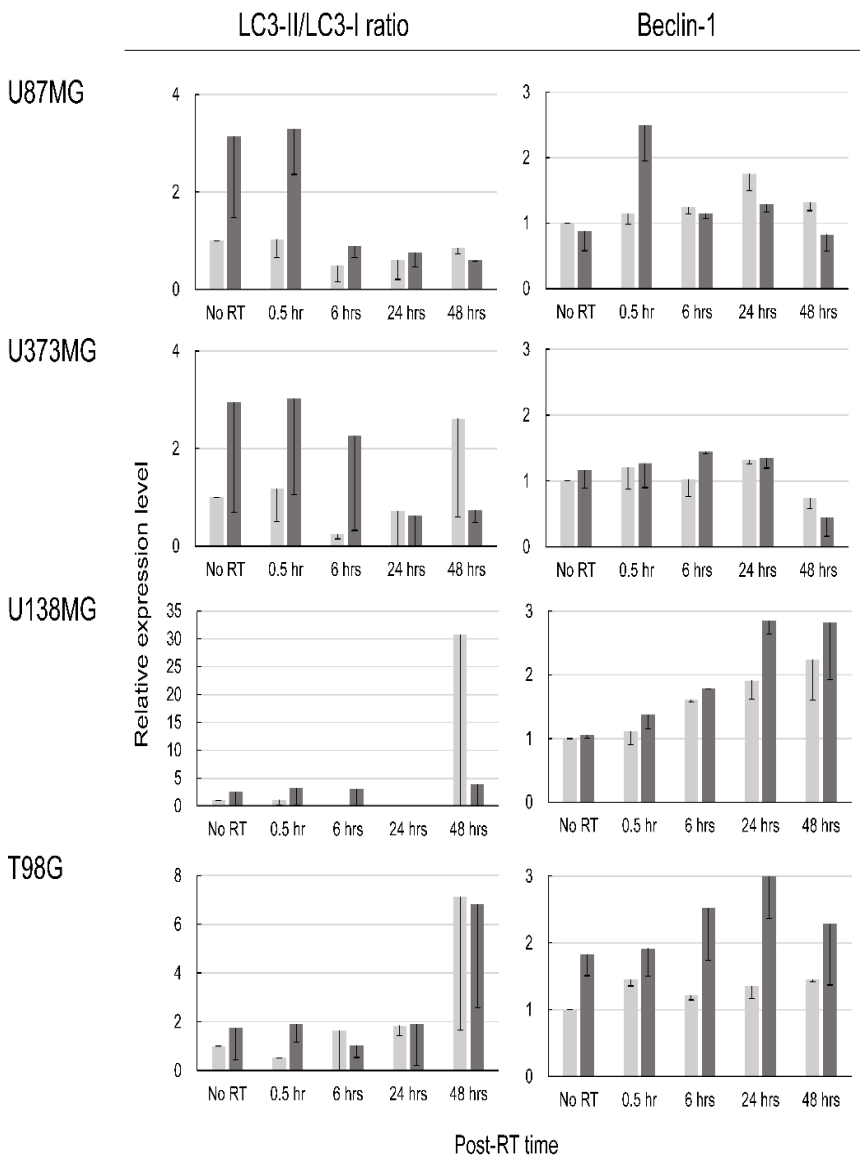
LC3-II/LC3-I ratio
Beclin-1
U87MG
U373MG
U138MG
T98G
Relative expression level
No RT
0.5 hr
6 hrs
24 hrs
48 hrs
Post-RT time

(B)

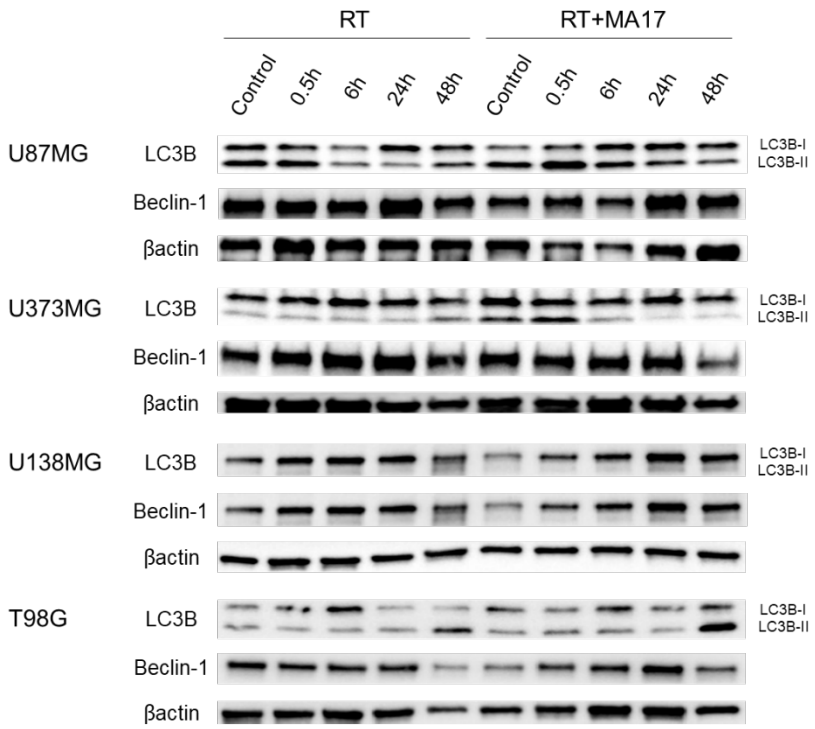

Figure 7. Western blot results for results of LC3-BII to LC3-BI ratio and of Beclin-1 expression normalized to β-actin in four glioblastoma cell lines treated with RT±MA17 shown as (A) densitometric analysis and (B) graphical protein expression bars. In U87MG and U373MG cells treated with RT+MA17, induction of autophagy was demonstrated represented as an increase in the LC3B-II to LC3B-I ratio at post-RT 0.5–6 hours compared to those treated with RT alone, whereas no difference in Beclin-1 expression was observed. In contrast, Beclin-1 expression was increased in U138MG and T98MG cells treated with RT+MA17 at post-RT 24–48 hours, whereas inconsistent changes of LC3B-II to LC3B-I ratio was observed in our study. RT, Radiotherapy. Light gray bar, RT; Dark gray bar, RT+MA17. Error bar: standard deviation.

5. Double-stranded DNA breaks

Changes in the proportion of cells harboring >10 γH2AX foci are shown in Figure 8 and Figure 9. The proportion of cells with double-stranded DNA breaks was similar between the treatment arms for the first 6 h post-RT, independent of MA17 treatment. However, during a later phase of 24–48 hours post-RT, a notably larger proportion of cells harbored >10 γH2AX foci if they had been treated with MA17, compared to those exposed to the RT treatment alone.

6. FANCA inhibition

In all four GBM cell lines, the expression of FANCA proteins was lower when they were treated with RT+MA17, compared to cells treated with RT alone (Figure 10). The difference was notable especially at post-RT 0.5 and 6 hours in all cell lines, but it progressively decreased thereafter. Interestingly, in U87MG and T98G cells, a significant inhibition of FANCA was sustained up to 48 hours post-RT.

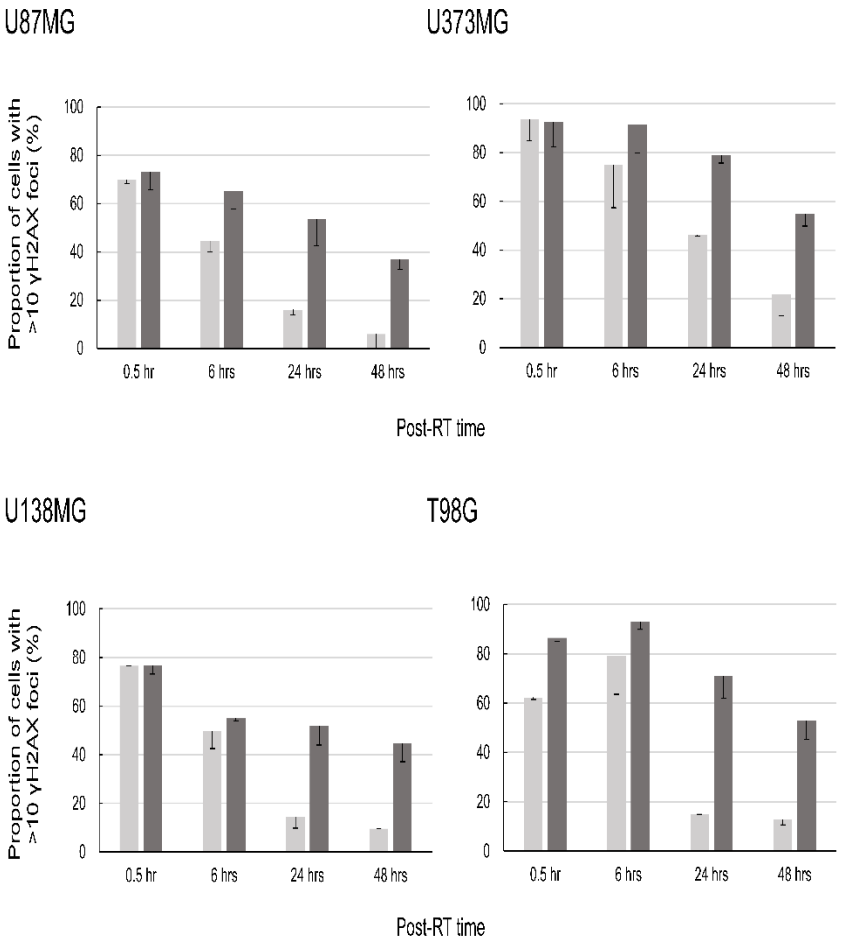

Figure 8. Immunocytochemistry results to evaluate changes in the proportion of cells harboring >10 γH2AX foci in four glioblastoma cell lines treated with RT±MA17. When cells treated by RT+MA17 vs. RT alone are compared, similar γ H2AX foci are observed during the post-RT 0.5–6-hours period. However, addition of MA17 to RT increased the proportion of cells harboring >10 γH2AX foci during the post-RT 24–48-hours period in all 4 glioblastoma cells, indicating delayed repair of RT-induced DNA double-strand breaks in cells treated by MA17. RT, Radiotherapy. Light gray bar, RT; Dark gray bar, RT+MA17. Error bar: standard deviation.

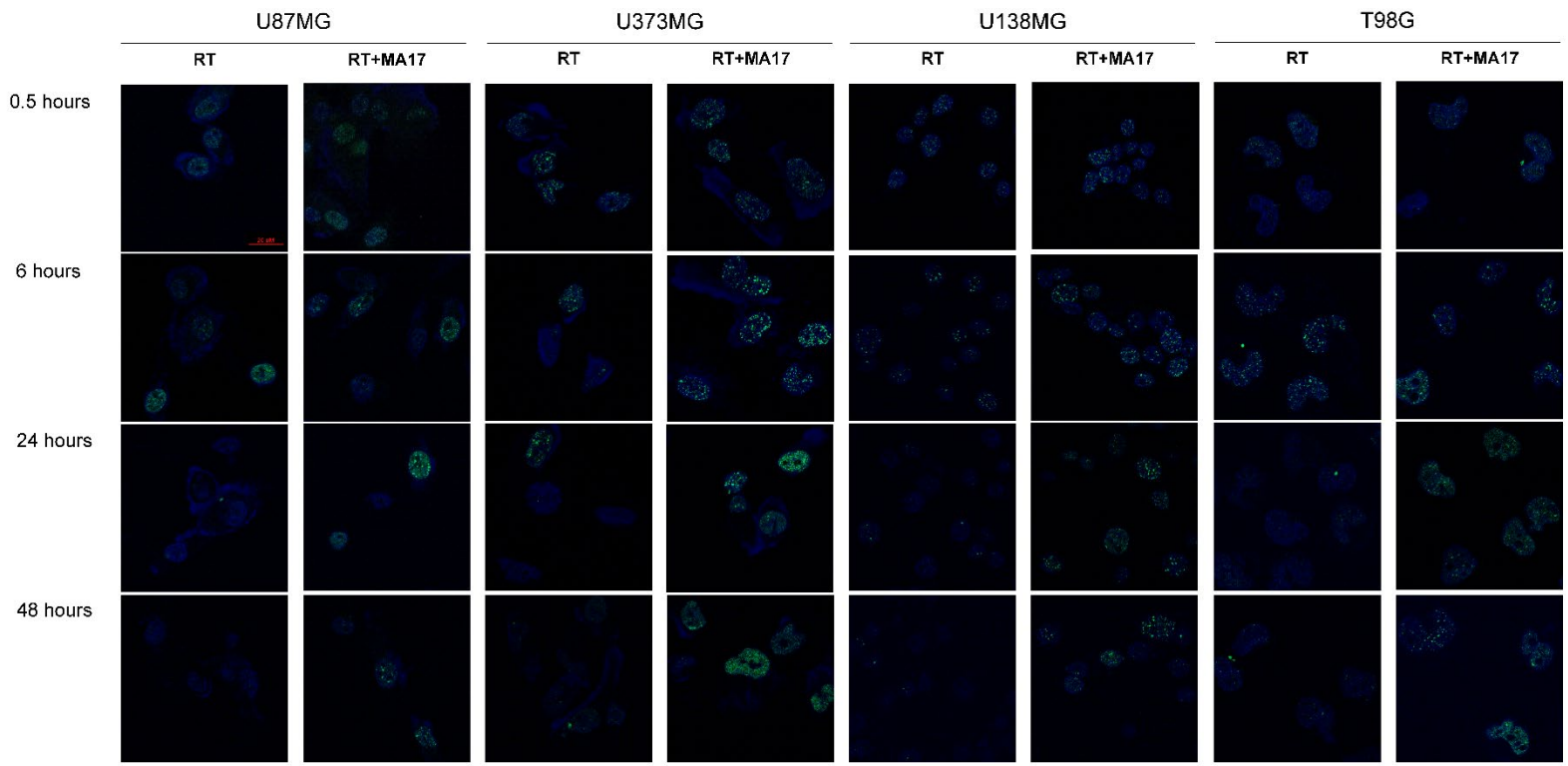
U87MG
U373MG
U138MG
T98G
RT
RT+MA17
RT
RT+MA17
RT
RT+MA17
RT
RT+MA17
0.5 hours
6 hours
24 hours
48 hours

Figure 9. Radiation-induced γH2AX foci. Representative micrographs were obtained from 4 glioblastoma cell lines treated by RT ±MA17. Cells harboring >10 γH2AX foci are significantly well visualized at post-RT 24–48 hours in cells treated with MA17 in all 4 glioblastoma cells. Blue fluorescence, DAPI; Green fluorescence, γH2AX.

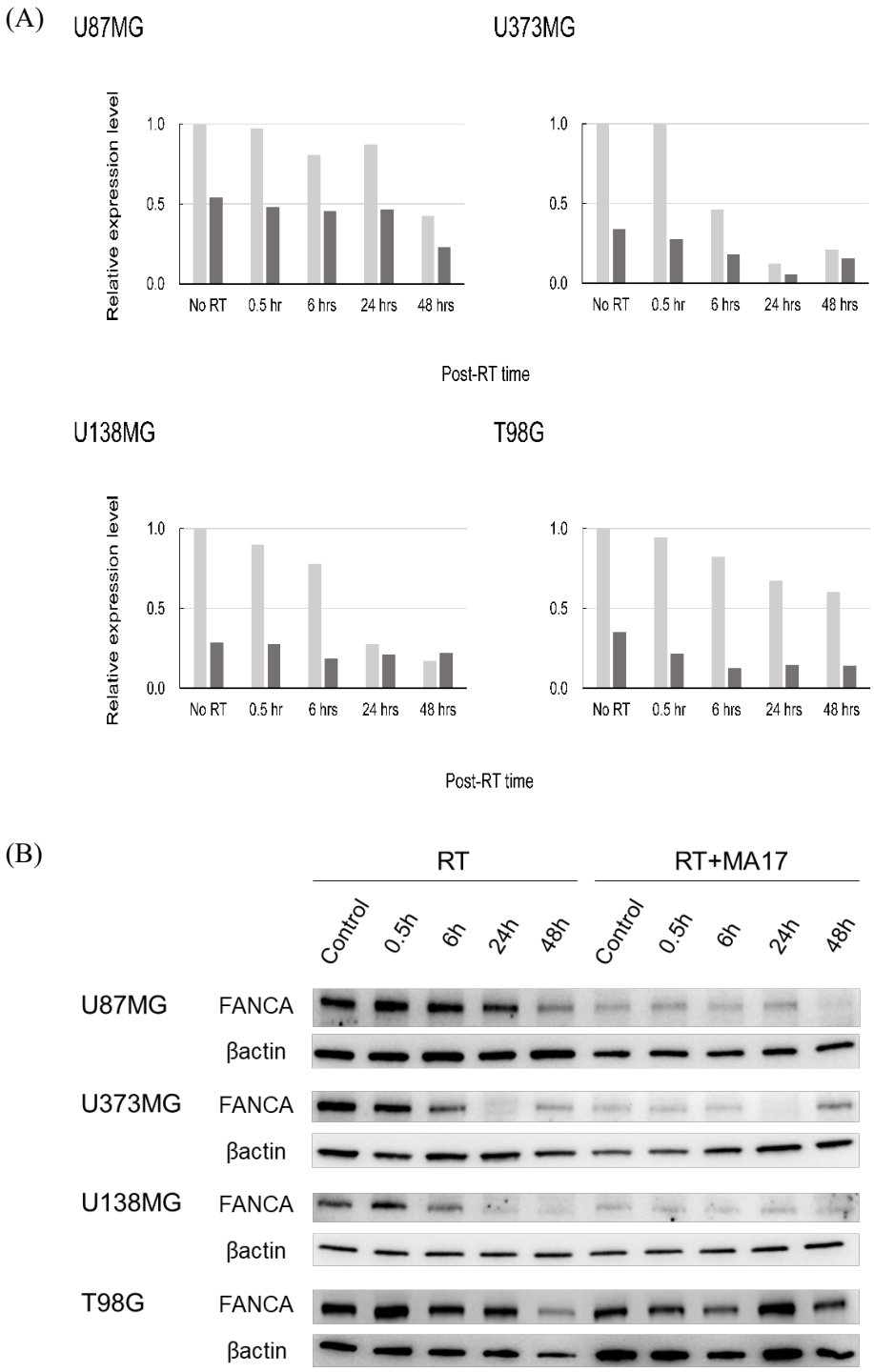

Figure 10. Western blot results of FANCA expression normalized to β-actin in four glioblastoma cell lines treated with RT±MA17 (n=1) shown as (A)

densitrometric analysis and (B) graphical protein expression bars. Compared to cells treated by RT alone, pretreatment with MA17 at a respective 50% inhibitory concentration in each cell line for 24 hours reduced the expression of FANCA proteins in all 4 glioblastoma cell lines. The reduction of FANCA expression was marked at post-RT 0.5–6 hours and decreased with time. RT, Radiotherapy. Light gray bar, RT; Dark gray bar, RT+MA17.

7. Tissue distribution of MA17 *in vivo*

The K_p obtained at 1.5 hours for brain, lung, testis, spleen, liver, and kidney were 'below limit of quantification', 0.93±0.57, 2.05±1.89, 1.06±1.08, 1.44±1.69, and 0.47±0.27, respectively (Figure 11).

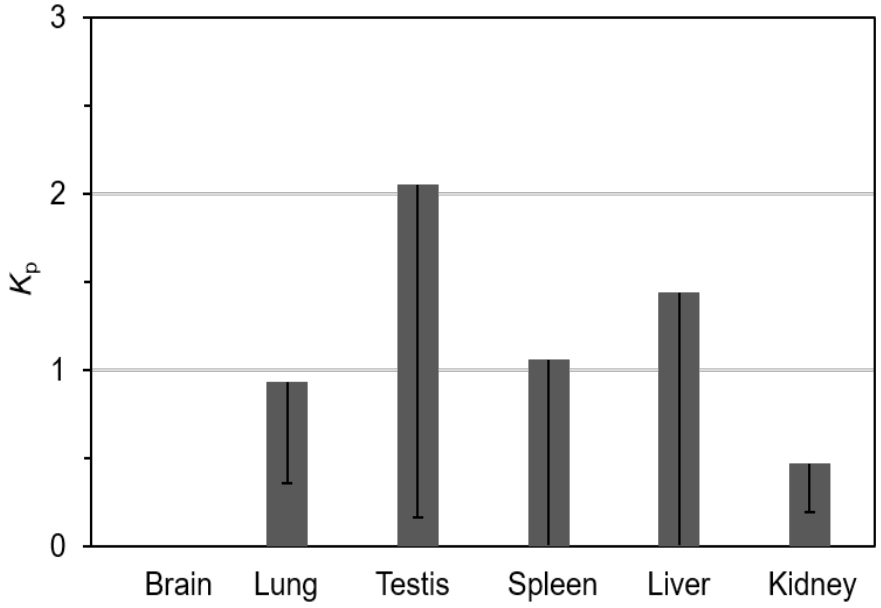

Figure 11. Tissue-to-plasma partition coefficient of MA17 *in vivo* (n=3). The tissue-to-plasma ratio (K_p), which is representative of tissue distribution of a compound, was obtained from brain, lung, testis, spleen, liver, and kidney for MA17 in ICR mice at post-injection 1.5 hours. The K_p in brain was 'below limit of quantification' whereas distribution of MA17 was observed to be high in the testes followed by liver, spleen, lung, and kidney. K_p, tissue-to-plasma partition coefficient.

8. KEGG pathway analysis

Using the ‘KEGG mapper’ we have successfully illustrated heatmaps of the five DNA repair pathways (base excision repair, mismatch repair, homologous recombination, nonhomologous end-joining, and Fanconi anemia pathway) based on the differentially expressed genes between cells treated with RT vs. RT+MA17 at post-RT 0.5, 6, and 24 hours (Figure 12). We could not identify any notably enriched or suppressed tendency during post-RT 0.5–24 hours regarding the base excision, mismatch repair, homologous recombination, and nonhomologous end-joining pathways (Figure 11A–D). Regarding the Fanconi anemia pathway, related genes were generally somewhat reduced in expression by MA17 at post-RT 6 hours, whereas, in contrast, the pathway seemed enriched at post-RT 24 hours by MA17 (Figure 11E).

(A) Base excision repair

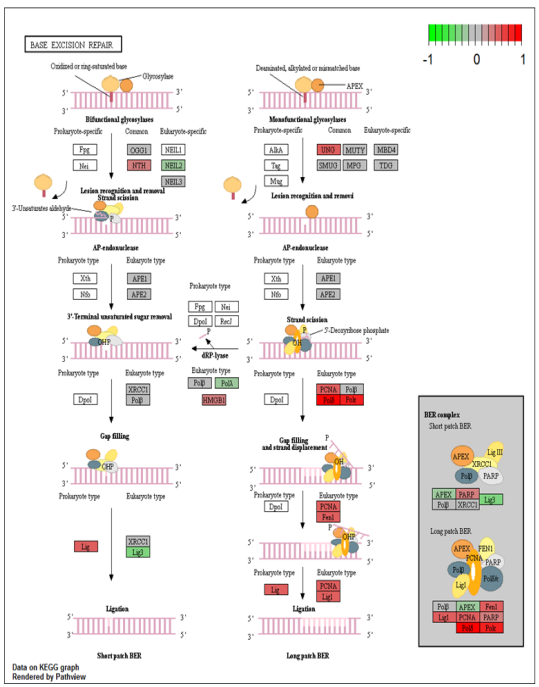

Post-RT 0.5h

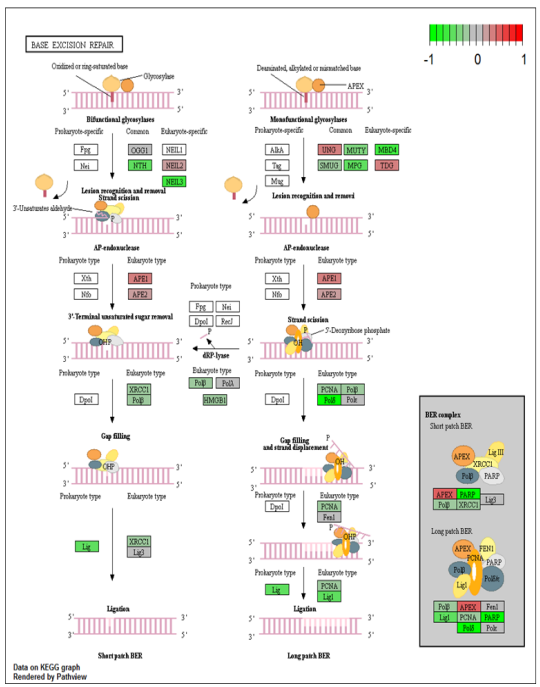

Post-RT 6h

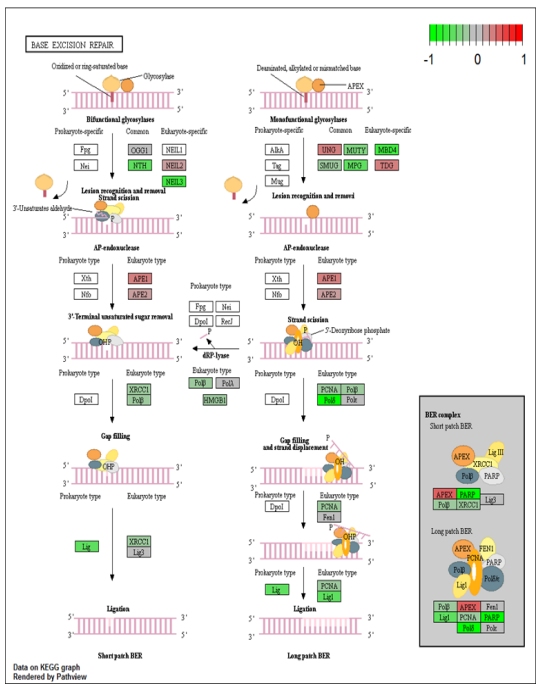

Post-RT 24h

(B) Mismatch repair

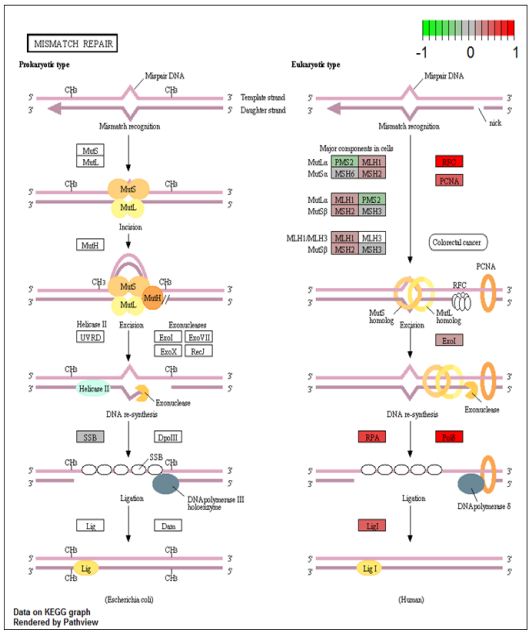

Post-RT 0.5h

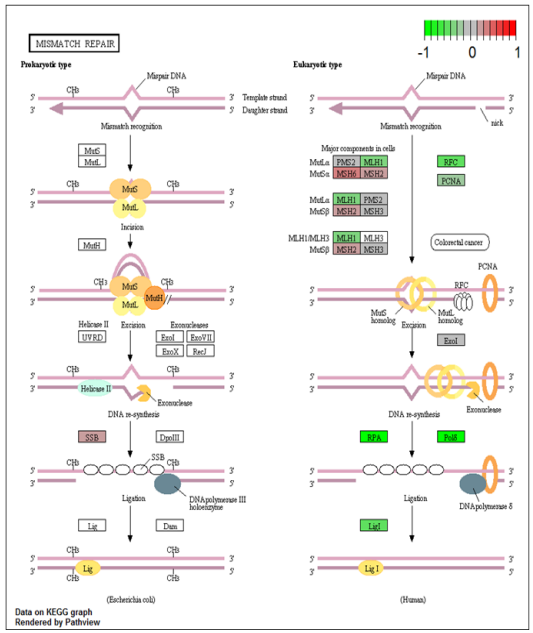

Post-RT 6h

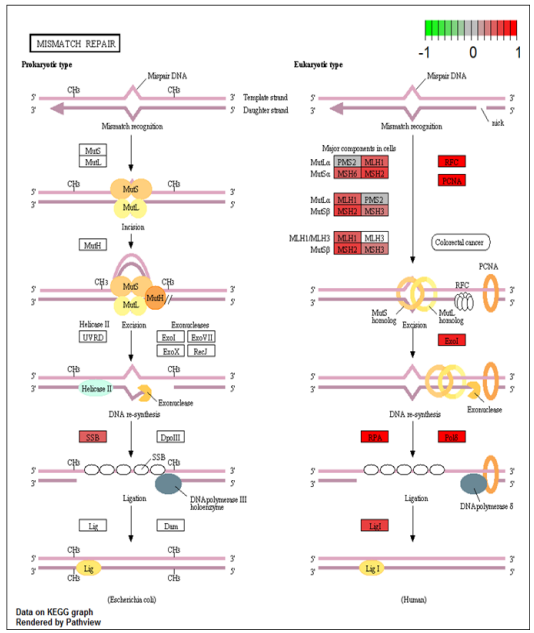

Post-RT 24h

(C) Homologous Recombination

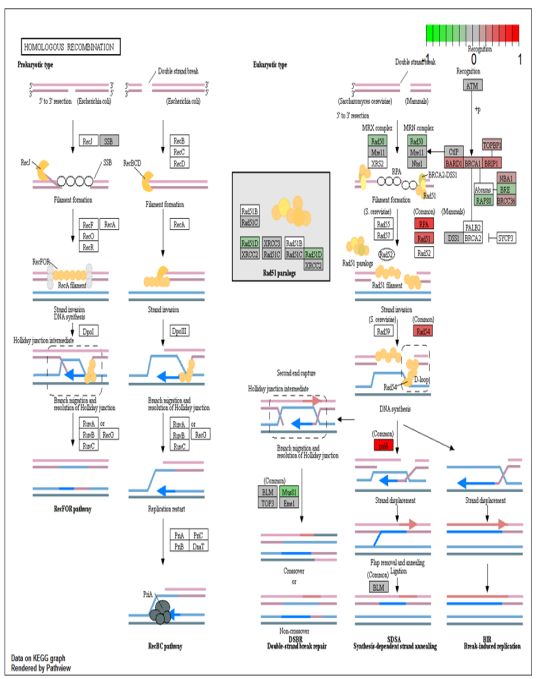

Post-RT 0.5h

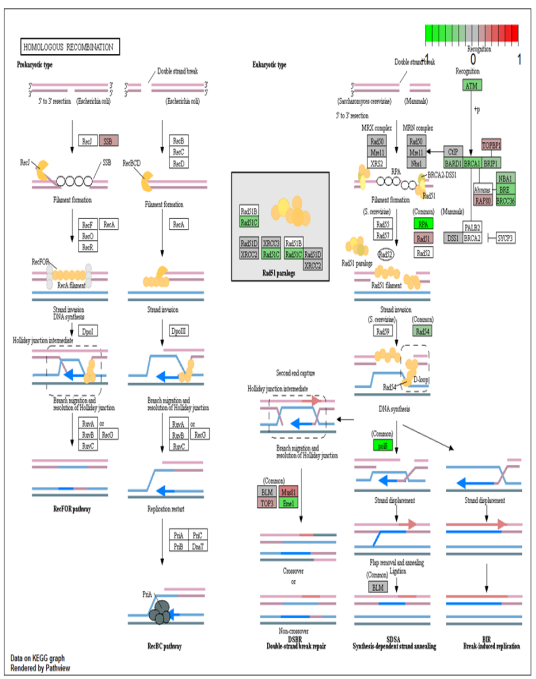

Post-RT 6h

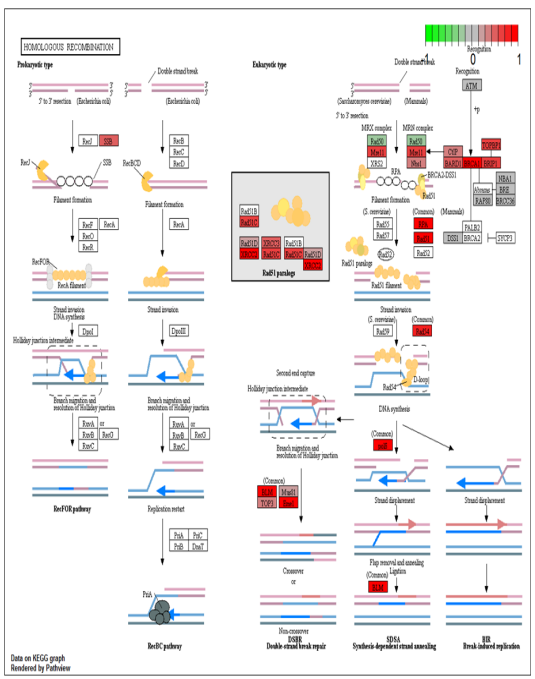

Post-RT 24h

(D) Non-homologous end-joining

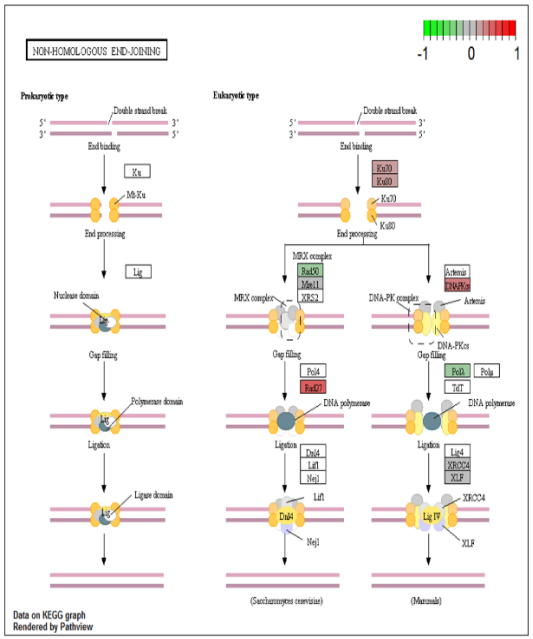

Post-RT 0.5h

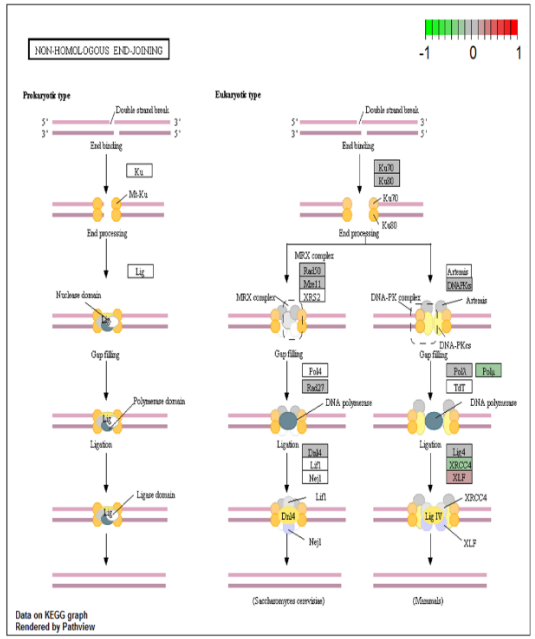

Post-RT 6h

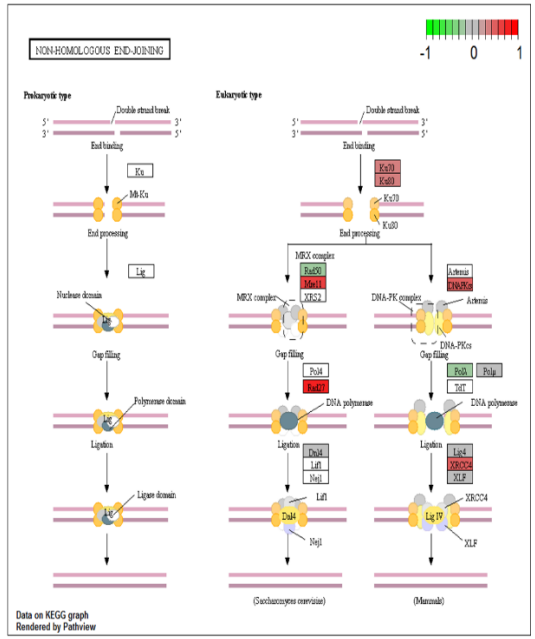

Post-RT 24h

(E) Fanconi anemia pathway

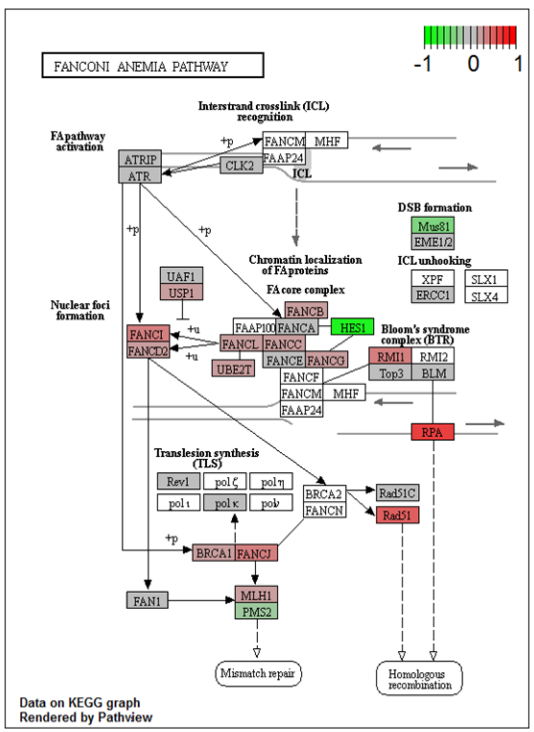

Post-RT 0.5h

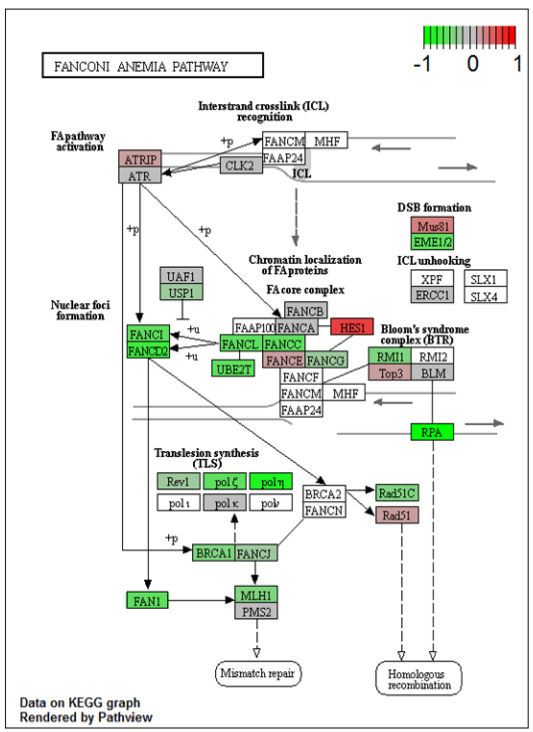

Post-RT 6h

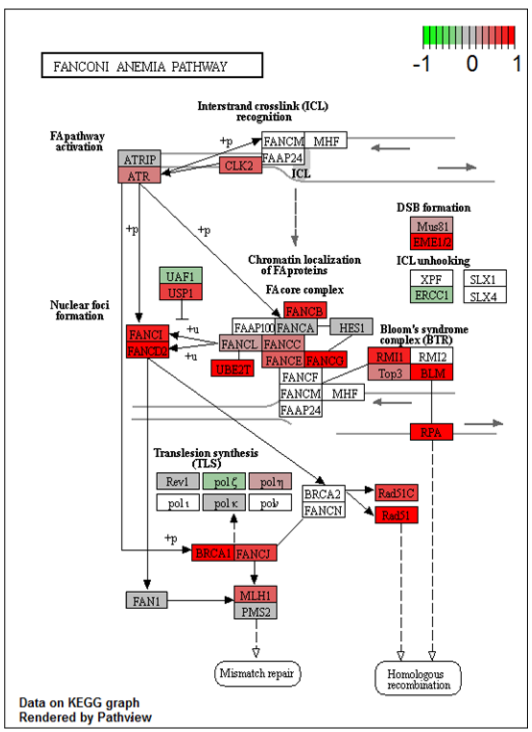

Post-RT 24h

Figure 12. The Kyoto Encyclopedia of Genes and Genomes analysis of the (A) base excision, (B) mismatch repair, (C) homologous recombination, (D) nonhomologous end-joining, and (E) Fanconi anemia pathways. No significant pathway enrichment by MA17 was observed during post-RT 0.5–24 hours regarding the (A) base excision, (B) mismatch repair, (C) homologous recombination, and (D) nonhomologous end-joining pathways. At post-RT 6 hours, the (E) Fanconi anemia pathway was slightly suppressed by MA17. However, the (E) Fanconi anemia pathway was inversely enriched at post-RT 24 hours by MA17. Log_2(fold change) is illustrated in colors: *Red*, increased gene expression by MA17; *Green*, reduced gene expression by MA17.

Discussion

GBM is the most common primary malignancy of the brain with one of the most notorious outcomes demonstrating a poor median survival of below 2 years (1–4). Although RT is a critical adjuvant treatment to improve survival most of the patients experience recurrence in the intensively irradiated areas (12, 13). Therefore, strategies that can enhance the tumoricidal efficacy of RT may be an extremely valuable strategy to overcome the devastating outcome of this disease. Development of radiosensitizers can enable an increase in the therapeutic window.

Since epigenetic change by DNA methylation plays a critical role in cancer development and aberrant growth of malignant cells, several DNMTis have been tested as direct anti-cancer drugs as well as potential radiosensitizing agents during the past decades in various cancer cells. Regarding radiosensitization, DNMTis have been tested in cancer cells of the brain, lung, colorectum, stomach, head and neck, pancreas, and prostate (23–27), and have demonstrated some promising results *in vitro*. Possible mechanisms of radiosensitization by DNMTis include the followings: i) inhibition of DNA repair process following RT, ii) decrease of the repopulation rate of cancer cells during RT by preferentially killing proliferative cells, and iii) induction of apoptosis in cancer cells (36). However, despite the optimistic *in vitro* results, their clinical use as radiosensitizers have been hampered by either their toxicity or poor biostability (28, 37). For example, in our previous study, a non-nucleoside DNMTi, psammaplin A, showed significant radiosensitizing effects in GBM and lung cancer cells by suppressing DNA repair (23). However, the

half-life of the agent in the mouse serum was under 10 minutes, limiting its clinical use in that form (28). This means that there is a huge need for novel DNMTis, which can sensitize cancer cells to RT without affecting normal tissues, and possess stability of a certain duration *in vivo*, in order to maximize the therapeutic effect of RT in its clinical application.

In our study, we evaluated a novel phthalimido-alkanamide derivative, as a DNMTi and as well as a radiosensitizer, using four different GBM cell lines. Colorimetric quantitative assay and western blot results revealed that MA17 is an inhibitor of DNMT1, DNMT3A, and DNMT3B. DNMT1 activity was suppressed by approximately 60% in the colorimetric assay by MA17. Pretreatment with MA17 for 24 hours also significantly enhanced the radiosensitivity of U87MG, U373MG, U138MG, and T98G cells with mean SERs of 1.196, 1.441, 1.152, and 1.350, respectively, *in vitro*. In contrast, MA17 did not show any evidence of radiosensization in the astrocytic NHA cells, demonstrating an ideal behavior as a radiosensitizer. Furthermore, *in vivo* study showed that MA17 does not distribute in the normal brain tissue at all (Figure 10) indicating that MA17 cannot cross the BBB successfully. This finding can be promising in regards of the therapeutic ratio of RT since the BBB is physically disrupted in areas of contrast enhancement on magnetic resonance imaging, the region which is usually the main target for RT. In contrast, normal brain tissues will not be affected by MA17 due to its poor BBB penetrance and since MA17 does not affect the radiosensitivity of normal astrocytes. A subsequent tumor growth delay assay, using the U87MG and U138MG cells, also revealed that injections of MA17 pre- or post-RT may generate a

significant delay in GBM cell growth *in vivo*, compared to those treated with RT alone and without MA17. Of note, it is very promising that MA17 has demonstrated significant radiosensitization even in GBM cells with unmethylated *MGMT* (U138MG), given their radioresistance and persistent survival (4, 20). However, it is yet clear from our results whether MA17 can even elevate the radiosensitivity when used in combination with RT/temozolomide. Subsequent experiments are necessary to compare the tumor growth in GBM cells when treated by RT+temozolomide+MA17 vs. RT+temozolomide.

The significant radiosensitization of GBM cells when treated with MA17 may be attributed to several different reasons. Firstly, the rate of apoptosis was increased in all four GBM cell lines treated with RT+MA17, as compared to cells treated with RT alone, although the timing and the magnitude of enhanced apoptosis differed between the different GBM cell lines we used. Apoptotic cell death is one of the major cell-killing mechanisms of RT (38), and it is well known that some DNMTis affect RT-induced apoptosis. For instance, Qiu et al. have reported that 5-aza-2'-deoxycytidine, a well-known DNMTi, enhanced RT-induced apoptosis in gastric cancer cells causing a cell cycle arrest at the G2-M phase (25). Kim et al. have also demonstrated that psammaplin A enhances RT-induced apoptosis in human lung cancer cells (23). Secondly, our results revealed that MA17 also enhances RT-induced autophagy in GBM cells. Autophagy is a critical process involved in cell death (39) and is known to be induced by RT in many types of cancers (40). Several studies have shown that combining drugs that enhance autophagy with RT, or even regulating genes

associated with autophagy, can enhance the radiosensitivity of cancer cells (40). Moreover, it is known that epigenetic alterations may affect the choice of cells for autophagic cell death (41). LC3-I to LC3-II conversion was dominantly seen in cells with *MGMT* methylation (U87MG and U373MG), whereas Beclin-1 function was dominantly elevated in cells without *MGMT* methylation. Further explanation for this difference is yet to be defined. Nevertheless, RT-induced autophagy was enhanced to some degree with the use of MA17 in all cell lines. Thirdly, double-stranded DNA break foci were observed for a prolonged period in cells treated with MA17 in addition to RT. The difference in proportion of cells possessing increased numbers of γH2AX foci was especially noted 24–48 hours post-RT in all four GBM cell lines. In a previous study from our group, the use of MA17 in addition to RT in human lung cancer cells, revealed that the Fanconi anemia pathway, which plays a critical role in repairing double-stranded DNA breaks (42), was significantly down-regulated when the RNA sequence data was analyzed (30). For this reason, we tested whether the expression of FANCA protein is down-regulated in GBM cells when these were pretreated with MA17. Indeed, the expression of FANCA was significantly lower in GBM cells receiving MA17, which probably contributed to the suppression of double-stranded DNA break repairs. Furthermore, based on the RNA sequencing data from U373MG cells treated by RT±MA17, we discovered a tendency of suppressed Fanconi anemia pathway at post-RT 6 hours. The decreased expression levels at the RNA level at post-RT 6 hours regarding the Fanconi anemia pathway might have affected the impaired DNA double-strand break repair during the following phase of post-RT 24–48 hours

confirmed in our study by γH2AX foci counts. Although the degree of suppression did not seem significant, this finding is in the context of the observation from our previous study by Kang et al., where the Fanconi anemia pathway was significantly suppressed by MA17 (30). However, in contrast to the finding by Kang et al. in lung cancer cells, we did not find any difference in the homologous recombination pathway between U373MG cells treated by RT alone or RT+MA17. Of note, at post-RT 24 hours, the Fanconi anemia pathway seemed to be unexpectedly enriched in U373MG cells treated with RT+MA17 compared to those treated with RT alone. This finding might have been due to diminished efficacy of MA17 after 24 hours and a following rebound reaction of frantic DNA double-strand break repair in cells with marked DNA double-strand breaks. Furthermore, this does not directly indicate that cell survival is superior in the cells treated by RT+MA17 at the period. Our RNA sequencing data possess several limitations since it was based on a single sample and was not confirmed in other cell lines such as U87MG, U138MG, and T98G. Nevertheless, FANCA protein expression was universally reduced in all 4 tested GBM cell lines in our study indicating impaired DNA repair as the mechanism of radiosensitization by MA17.

Several obstacles need to be surmounted for this novel phthalimido-alkanamide derivative to be tested in clinical trials for GBM patients. The agent is highly lipophilic and has shown low solubility in saline. As a consequence, MA17 was injected in mice after being dissolved in DMSO, an agent associated with neurotoxicity (43). Furthermore, although injected intraperitoneally, the exact concentration of the drug as well as other pharmacokinetic parameters in

the serum, brain tissue, and tumor of the mice were not examined in our study. Therefore, the proper form and route of the drug administration as well as the optimal concentration for use still needs to be determined. Although poor BBB penetrance may be beneficial to target contrast-enhancing lesions, efforts must be made to improve BBB penetrance of MA17 for non-enhancing infiltrative tumor, often presenting with T2 high signal intensity on magnetic resonance imaging (44). Although there was no unexpected mortality or significant weight loss following treatment *in vivo* in our study, the toxicity profiles of the drug also need to be evaluated thoroughly. Furthermore, although MA17 did not affect the sensitivity to RT in NHA cells, and non-nucleoside DNMTis are less toxic compared to nucleosides in general, the drug might con unexpected toxicity of the drug may be encountered. However, the weight loss of approximately 1g in U87MG-harboring mice during the first 3 days following treatment is considered nonspecific since almost no weight loss was observed in U138MG-harboring mice during the identical period. In our hands, no severe acute toxicity seemed to occur in mice after administration of MA17 during the follow-up period.

In summary, we used a newly synthesized compound that exhibits significant radiosensitizing effects in GBM cells without affecting normal astrocytes. Apoptosis, autophagy, and suppression of DNA repair is enhanced by this agent in combination with RT, and those are the possible mechanisms of radiosensitization. Several limitations for clinical application of the drug still exist. Nevertheless, this novel compound brightens the prospects of treating GBM, which is currently regarded as an incurable type of cancer.

Reference

[1] Ostrom QT, Gittleman H, Truitt G, Boscia A, Kruchko C and Barnholtz-Sloan JS. CBTRUS Statistical Report: Primary Brain and Other Central Nervous System Tumors Diagnosed in the United States in 2011-2015. Neuro Oncol 20(suppl_4): iv1–iv86, 2018.

[2] Walker MD, Alexander E Jr, Hunt WE, MacCarty CS, Mahaley MS Jr, Mealey J Jr, Norrell HA, Owens G, Ransohoff J, Wilson CB, Gehan EA and Strike TA. Evaluation of BCNU and/or radiotherapy in the treatment of anaplastic gliomas. A cooperative clinical trial. J Neurosurg 49(3): 333–43, 1978.

[3] Stupp R, Mason WP, van den Bent MJ, Weller M, Fisher B, Taphoorn MJ, Belanger K, Brandes AA, Marosi C, Bogdahn U, Curschmann J, Janzer RC, Ludwin SK, Gorlia T, Allgeier A, Lacombe D, Cairncross JG, Eisenhauer E and Mirimanoff RO: Radiotherapy plus concomitant and adjuvant temozolomide for glioblastoma. N Engl J Med 352(10): 987–96, 2005.

[4] Wee CW, Kim E, Kim N, Kim IA, Kim TM, Kim YJ, Park CK, Kim JW, Kim CY, Choi SH, Kim JH, Park SH, Choe G, Lee ST, Chang JH, Kim SH, Suh CO and Kim IH: Novel recursive partitioning analysis classification for newly diagnosed glioblastoma: A multi-institutional study highlighting the MGMT promoter methylation and IDH1 gene mutation status. Radiother Oncol 123(1): 106–11, 2017.

[5] Perry JR, Laperriere N, O'Callaghan CJ, Brandes AA, Menten J, Phillips C, Fay M, Nishikawa R, Cairncross JG, Roa W, Osoba D, Rossiter JP, Sahgal A, Hirte H, Laigle-Donadey F, Franceschi E, Chinot O,

Golfinopoulos V, Fariselli L, Wick A, Feuvret L, Back M, Tills M, Winch C, Baumert BG, Wick W, Ding K and Mason WP. Short-Course Radiation plus Temozolomide in Elderly Patients with Glioblastoma. N Engl J Med 376(11): 1027–37, 2017.

[6] Gilbert MR, Wang M, Aldape KD, Stupp R, Hegi ME, Jaeckle KA, Armstrong TS, Wefel JS, Won M, Blumenthal DT, Mahajan A, Schultz CJ, Erridge S, Baumert B, Hopkins KI, Tzuk-Shina T, Brown PD, Chakravarti A, Curran WJ Jr and Mehta MP. Dose-dense temozolomide for newly diagnosed glioblastoma: a randomized phase III clinical trial. J Clin Oncol 31(32): 4085–91, 2013.

[7] Gilbert MR, Dignam JJ, Armstrong TS, Wefel JS, Blumenthal DT, Vogelbaum MA, Colman H, Chakravarti A, Pugh S, Won M, Jeraj R, Brown PD, Jaeckle KA, Schiff D, Stieber VW, Brachman DG, Werner-Wasik M, Tremont-Lukats IW, Sulman EP, Aldape KD, Curran WJ Jr and Mehta MP. A randomized trial of bevacizumab for newly diagnosed glioblastoma. N Engl J Med 370(8): 699–708, 2014.

[8] Bao S, Wu Q, McLendon RE, Hao Y, Shi Q, Hjelmeland AB, Dewhirst MW, Bigner DD and Rich JN: Glioma stem cells promote radioresistance by preferential activation of the DNA damage response. Nature 444(7120): 756–60, 2006.

[9] Minata M, Audia A, Shi J, Lu S, Bernstock J, Pavlyukov MS, Das A, Kim SH, Shin YJ, Lee Y, Koo H, Snigdha K, Waghmare I, Guo X, Mohyeldin A, Gallego-Perez D, Wang J, Chen D, Cheng P, Mukheef F, Contreras M, Reyes JF, Vaillant B, Sulman EP, Cheng SY, Markert JM, Tannous BA, Lu

X, Kango-Singh M, Lee LJ, Nam DH, Nakano I and Bhat KP. Phenotypic Plasticity of Invasive Edge Glioma Stem-like Cells in Response to Ionizing Radiation. Cell Rep 26(7): 1893–905, 2019.

[10] Lin JC, Tsai JT, Chao TY, Ma HI, Chien CS and Liu WH. MSI1 associates glioblastoma radioresistance via homologous recombination repair, tumor invasion and cancer stem-like cell properties. Radiother Oncol 129(2): 352–63, 2018.

[11] Brandes AA, Tosoni A, Franceschi E, Sotti G, Frezza G, Amistà P, Morandi L, Spagnolli F and Ermani M. Recurrence pattern after temozolomide concomitant with and adjuvant to radiotherapy in newly diagnosed patients with glioblastoma: correlation With MGMT promoter methylation status. J Clin Oncol 27(8): 1275–9, 2009.

[12] Minniti G, Amelio D, Amichetti M, Salvati M, Muni R, Bozzao A, Lanzetta G, Scarpino S, Arcella A and Enrici RM: Patterns of failure and comparison of different target volume delineations in patients with glioblastoma treated with conformal radiotherapy plus concomitant and adjuvant temozolomide. Radiother Oncol 97(3): 377–81, 2010.

[13] Chang EL, Akyurek S, Avalos T, Rebueno N, Spicer C, Garcia J, Famiglietti R, Allen PK, Chao KS, Mahajan A, Woo SY and Maor MH. Evaluation of peritumoral edema in the delineation of radiotherapy clinical target volumes for glioblastoma. Int J Radiat Oncol Biol Phys 68(1): 144–50, 2007.

[14] Jones PA and Baylin SB: The epigenomics of cancer. Cell 128(4): 683–92, 2007.

[15] Rodriguez-Paredes M and Esteller M: Cancer epigenetics reaches mainstream oncology. Nat Med 17(3): 330–9, 2011.

[16] van Engeland M, Derks S, Smits KM, Meijer GA and Herman JG: Colorectal cancer epigenetics: complex simplicity. J Clin Oncol 29(10): 1382–91, 2011.

[17] Feinberg AP and Tycko B: The history of cancer epigenetics. Nat Rev Cancer 4(2): 143–53, 2004.

[18] Amatya VJ, Naumann U, Weller M and Ohgaki H: TP53 promoter methylation in human gliomas. Acta Neuropathol 110(2): 178–84, 2005.

[19] Nakamura M, Yonekawa Y, Kleihues P and Ohgaki H: Promoter hypermethylation of the RB1 gene in glioblastomas. Lab Invest 81(1): 77–82, 2001.

[20] Hegi ME, Diserens AC, Gorlia T, Hamou MF, de Tribolet N, Weller M, Kros JM, Hainfellner JA, Mason W, Mariani L, Bromberg JE, Hau P, Mirimanoff RO, Cairncross JG, Janzer RC and Stupp R: MGMT gene silencing and benefit from temozolomide in glioblastoma. N Engl J Med 352(10): 997–1003, 2005.

[21] Noushmehr H, Weisenberger DJ, Diefes K, Phillips HS, Pujara K, Berman BP, Pan F, Pelloski CE, Sulman EP, Bhat KP, Verhaak RG, Hoadley KA, Hayes DN, Perou CM, Schmidt HK, Ding L, Wilson RK, Van Den Berg D, Shen H, Bengtsson H, Neuvial P, Cope LM, Buckley J, Herman JG, Baylin SB, Laird PW and Aldape K. Identification of a CpG island methylator phenotype that defines a distinct subgroup of glioma. Cancer Cell 17(5): 510–22, 2010.

[22] Wouters BJ and Delwel R. Epigenetics and approaches to targeted epigenetic therapy in acute myeloid leukemia. Blood 127(1): 42–52, 2016.

[23] Kim HJ, Kim JH, Chie EK, Young PD, Kim IA and Kim IH: DNMT (DNA methyltransferase) inhibitors radiosensitize human cancer cells by suppressing DNA repair activity. Radiat Oncol 7: 39, 2012.

[24] Hofstetter B, Niemierko A, Forrer C, Benhattar J, Albertini V, Pruschy M, Bosman FT, Catapano CV and Ciernik IF: Impact of genomic methylation on radiation sensitivity of colorectal carcinoma. Int J Radiat Oncol Biol Phys 76(5): 1512–9, 2010.

[25] Qiu H, Yashiro M, Shinto O, Matsuzaki T and Hirakawa K: DNA methyltransferase inhibitor 5-aza-CdR enhances the radiosensitivity of gastric cancer cells. Cancer Sci 100(1): 181-8, 2009.

[26] De Schutter H, Kimpe M, Isebaert S and Nuyts S: A systematic assessment of radiation dose enhancement by 5-Aza-20-deoxycytidine and histone deacetylase inhibitors in head-and-neck squamous cell carcinoma. Int J Radiat Oncol Biol Phys 73(3): 904–12, 2009.

[27] Dote H, Cerna D, Burgan WE, Carter DJ, Cerra MA, Hollingshead MG, Camphausen K and Tofilon PJ: Enhancement of in vitro and in vivo tumor cell radiosensitivity by the DNA methylation inhibitor zebularine. Clin Cancer Res 11(12): 4571–9, 2005.

[28] Kim HJ, Kim TH, Seo WS, Yoo SD, Kim IH, Joo SH, Shin S, Park ES, Ma ES and Shin BS: Pharmacokinetics and tissue distribution of psammaplin A, a novel anticancer agent, in mice. Arch Pharm Res 35(10): 1849–54, 2012.

[29] Wee CW, Kim JH, Kim HJ, Kang HC, Suh SY, Shin BS, Ma E and Kim IH. Psammaplin A-Modified Novel Radiosensitizers for Human Lung Cancer and Glioblastoma Cells. J Radiat Prot Res 44(1): 15–25, 2019.

[30] Kang HC, Chie EK, Kim HJ, Kim JH, Kim IH, Kim K, Shin BS and Ma E. A phthalimidoalkanamide derived novel DNMT inhibitor enhanced radiosensitivity of A549 cells by inhibition of homologous recombination of DNA damage. Invest New Drugs 2019. doi: 10.1007/s10637-019-00730-6 [Epub ahead of print].

[31] Alonso MM, Gomez-Manzano C, Bekele BN, Yung WK and Fueyo J: Adenovirus-based strategies overcome temozolomide resistance by silencing the O6-methylguanine-DNA methyltransferase promoter. Cancer Res 67(24): 11499–504, 2007.

[32] Gaspar N, Marshall L, Perryman L, Bax DA, Little SE, Viana-Pereira M, Sharp SY, Vassal G, Pearson AD, Reis RM, Hargrave D, Workman P and Jones C: MGMT-independent temozolomide resistance in pediatric glioblastoma cells associated with a PI3-kinase-mediated HOX/stem cell gene signature. Cancer Res 70(22): 9243–52, 2010.

[33] Li S, Chou AP, Chen W, Chen R, Deng Y, Phillips HS, Selfridge J, Zurayk M, Lou JJ, Everson RG, Wu KC, Faull KF, Cloughesy T, Liau LM and Lai A: Overexpression of isocitrate dehydrogenase mutant proteins renders glioma cells more sensitive to radiation. Neuro Oncol 15(1): 57–68, 2013.

[34] Klionsky DJ, Cuervo AM and Seglen PO: Methods for monitoring autophagy from yeast to human. Autophagy 3(3): 181–206, 2007.

[35] Walden H and Deans AJ: The Fanconi anemia DNA repair pathway:

structural and functional insights into a complex disorder. Annu Rev Biophys 43: 257–78, 2014.

[36] Smits KM, Melotte V, Niessen HE, Dubois L, Oberije C, Troost EG, Starmans MH, Boutros PC, Vooijs M, van Engeland M and Lambin P: Epigenetics in radiotherapy: where are we heading? Radiother Oncol 111(2): 168–77, 2014.

[37] Aparicio A and Weber JS: Review of the clinical experience with 5-azacytidine and 5-aza-2′-deoxycytidine in solid tumors. Curr Opin Investig Drugs 3(4): 627–33, 2002.

[38] Dewey WC, Ling CC and Meyn RE: Radiation-induced apoptosis: relevance to radiotherapy. Int J Radiat Oncol Biol Phys 33(4): 781–96, 1995.

[39] Ito H, Daido S, Kanzawa T, Kondo S and Kondo Y: Radiation-induced autophagy is associated with LC3 and its inhibition sensitizes malignant glioma cells. Int J Oncol 26(5): 1401–10, 2005.

[40] Xin Y, Jiang F, Yang C, Yan Q, Guo W, Huang Q, Zhang L and Jiang G: Role of autophagy in regulating the radiosensitivity of tumor cells. J Cancer Res Clin Oncol 143(11): 2147–57, 2017.

[41] Sui X, Zhu J, Zhou J, Wang X, Li D, Han W, Fang Y and Pan H: Epigenetic modifications as regulatory elements of autophagy in cancer. Cancer Lett 360(2): 106–13, 2015.

[42] Michl J, Zimmer J and Tarsounas M: Interplay between Fanconi anemia and homologous recombination pathways in genome integrity. EMBO J 35(9): 909–923, 2016.

[43] Yuan C, Gao J, Guo J, Bai L, Marshall C, Cai Z, Wang L and Xiao M: Dimethyl sulfoxide damages mitochondrial integrity and membrane potential in cultured astrocytes. PLoS One 9(9): e107447, 2014.

[44] Sarkaria JN, Hu LS, Parney IF, Pafundi DH, Brinkmann DH, Laack NN, Giannini C, Burns TC, Kizilbash SH, Laramy JK, Swanson KR, Kaufmann TJ, Brown PD, Agar NYR, Galanis E, Buckner JC and Elmquist WF. Is the blood-brain barrier really disrupted in all glioblastomas? A critical assessment of existing clinical data. Neuro Oncol 2018; 20(2): 184–191.

국문초록

교모세포종 세포주 및 이식종양 모델에서 DNA Methyltransferase 억제제인
신합성 Phthalimido-alkanamide 유도체의 방사선감수성 증강효과 및 기전

위찬우
서울대학교 대학원
의학과 방사선종양학 전공

배경 및 목적: 교모세포종은 성인에서 가장 흔한 원발성 뇌종양이다. 하지만 핵심적 치료기법인 수술-방사선요법의 발전에도 불구하고 예후는 극히 불량하다. 이에 본 연구를 통해 DNA methyltransferase를 억제하는 십합성 phthalimido-alkanamide 유도체가 교모세포종에서 세포에서 방사선감수성 증강 효과가 있는지 및 그 기전이 무엇인지를 규명하기로 하였다.

방법: 총 4종류의 인간 교모세포종 세포주(U87MG, U373MG, U138MG, T98G)와 1종류의 인간 정상 별아교세포 세포주(NHA)를 배양하여 사용하였다. 신합성된 phthalimido-alkanamide 유도체인 MA17의 방사선감작효과는 세포집락형성능력을 기준으로 한 세포생존을 기본지표로 평가하였다. 방사선은 6MV 엑스선을 사용하였고 약물병용시에는 MA17을 방사선조사전 24시간동안 전처치하였다. 또한 방사선감작의 기전을 규명하기 위하여 DNA methyltransferase의 (DNMT) 억제, 세포고사, 자가포식, DNA 손상 회복, FANCA 발현 정도를 측정하였다. 모든 *in vitro* 실험은 독립적으로 3회

실시하였다. *In vivo*에서 방사선감작효과를 평가하기 위하여 2종류의 세포주를 (U87MG와 U138MG) BALB/C-nude 마우스의 등에 이식하였고, 방사선조사후 종양성장지연측정 방법을 통하여 MA17의 *in vivo* 방사선감작효과를 평가하였다. 또한 MA17이 혈뇌장벽을 통과하여 뇌조직에 분포할 수 있는지를 평가하기 위해 조직-혈장 분배계수를 측정하였다.

결과: *In vitro*에서 MA17은 4종류의 교모세포종 세포주 모두에서 유의한 방사선감작효과를 나타내었다. 생존분획 0.2에서의 평균 방사선효과증강율은 U87MG, U373MG, U138MG, T98G 세포에서 각각 1.196 ($p=0.034$), 1.441 ($p=0.029$), 1.152 ($p=0.030$), 1.350이었다 ($p<0.001$). 그러나 MA17은 정상 별아교세포 세포주에서는 평균 방사선효과증강율 1.016으로 ($p=0.420$) 방사선민감도에 영향을 주지 않았다. *In vivo* 종양성장지연측정 실험에서도 방사선조사와 MA17을 병용한 군에서 방사선조사 단독군에 비하여 종양배가시간이 U87MG과 U138MG 종양에서 각각 6.35일과 ($p=0.009$) 3.06일씩 ($p=0.030$) 증가하였다. Western blot에서는 MA17이 DNMT1/DNMT3A/DNMT3B 활동도를 저해하고 세포고사 및 자가포식를 유도한다는 것을 확인하였다. 또한 MA17에 의해 4종류의 교모세포종 세포주에서 DNA 이중가닥 절단의 복구가 지연되고 및 FANCA 단백질 발현이 억제됨을 확인하였다. MA17의 조직-혈장 분배계수는 검출한계 미만으로 도출되어, MA17은 혈뇌장벽을 통과하여 뇌조직에 분포하지 않는 것으로 나타났다.

결론: 본 연구는 교모세포종에서 신합성 phthalimido-alkanamide 유도체인 MA17이 지닌 방사선감작효과를 확인한 첫번째 연구이다.

*In vitro*와 *in vivo* 모두에서 MA17은 유의한 방사선감작효과를 보였다. 그 기전으로는 MA17에 의한 세포고사 및 자가포식 유발과 DNA 손상회복 및 FANCA 단백질 발현억제 등이 관여하는 것으로 확인되었다. 이 신약의 임상적용은 추가연구가 필요할 것으로 보인다.

주요어: DNA methyltransferase, 방사선조사, 방사선감작제, 교모세포종, phthalimido-alkanamide

학 번: 2014-21992